



Contents lists available at SciVerse ScienceDirect

Atomic Data and Nuclear Data Tables

journal homepage: www.elsevier.com/locate/adt

Table of experimental nuclear ground state charge radii: An update

I. Angeli^a, K.P. Marinova^{b,*}^a Institute of Experimental Physics, University of Debrecen, H-4010 Debrecen Pf. 105, Hungary^b Joint Institute for Nuclear Research, 141980 Dubna, Moscow Region, Russia

ARTICLE INFO

Article history:

Received 9 August 2011

Received in revised form

10 November 2011

Accepted 2 December 2011

Available online 12 December 2012

Keywords:

Nuclear charge radii

Radii changes

Optical isotope shifts

 K_{α} X-ray isotope shifts

Electron scattering

Muonic atom spectra

ABSTRACT

The present table contains experimental root-mean-square (*rms*) nuclear charge radii R obtained by combined analysis of two types of experimental data: (i) radii changes determined from optical and, to a lesser extent, K_{α} X-ray isotope shifts and (ii) absolute radii measured by muonic spectra and electronic scattering experiments. The table combines the results of two working groups, using respectively two different methods of evaluation, published in ADNDT earlier. It presents an updated set of *rms* charge radii for 909 isotopes of 92 elements from ${}^1\text{H}$ to ${}^{96}\text{Cm}$ together, when available, with the radii changes from optical isotope shifts. Compared with the last published tables of R -values from 2004 (799 ground states), many new data are added due to progress recently achieved by laser spectroscopy up to early 2011. The radii changes in isotopic chains for He, Li, Be, Ne, Sc, Mn, Y, Nb, Bi have been first obtained in the last years and several isotopic sequences have been recently extended to regions far off stability, (e.g., Ar, Mo, Sn, Te, Pb, Po).

© 2012 Elsevier Inc. All rights reserved.

* Corresponding author. Tel.: +7 4962162084; fax: +7 49621 65083.

E-mail address: marinova@nrmail.jinr.ru (K.P. Marinova).

Contents

1. Introduction.....	70
2. Evaluation procedures.....	70
3. Data sources.....	71
3.1. Radii changes from optical isotope shift.....	71
3.2. Radii differences between isotopes from K_α isotope shifts.....	72
3.3. rms radii from e^- and μ^- experiments.....	72
4. Global behaviour of rms nuclear charge radii.....	73
Acknowledgments.....	75
References.....	75
Explanation of Tables.....	76
Table 1. Nuclear radii changes and rms nuclear charge radii.....	76
Table 2. Parameters used for extraction of radii changes from OIS.....	76

1. Introduction

The nuclear charge radius is one of the most obvious and important nuclear parameters that give information about the nuclear shell model and the influence of effective interactions on nuclear structure. Experimental information on root-mean-square (rms) nuclear charge radii can be derived from different sources and has been published several times. The results from electron scattering (e^-) experiments are expressed in terms of the rms radius, and, for some nuclei, in parameters of the Fermi-distribution [1,2]. Muonic X-ray energies are another source of information. These probe somewhat different moments of nuclear distribution, the so called “Barrett moments” $\langle r^k e^{-ar} \rangle$, nevertheless the results are quoted also in terms of $\langle r^2 \rangle$ [3,4]. Optical and K_α X-ray isotope shifts are sensitive to the same nuclear parameters and provide an important source of complementary information on mean square (ms) radii changes $\delta\langle r^2 \rangle$. The K_α X results are easier to interpret; however, these measurements can be performed only on stable isotopes since the experimental method requires several tens of milligrams of target. The same refers to experiments with μ^- atoms and electron scattering e^- , while optical isotope shifts (OIS) can be measured with negligible quantities of radioactive atoms, inclusive single ones, with lifetimes down to 1 ms, and thus give access to long chains of radioactive isotopes extending far off stability [5,6].

The four electromagnetic methods are sensitive to different properties of the nuclear ground-state charge distributions. For this reason, a combination of data from different experimental methods generally yields more detailed and accurate knowledge of the nuclear radii than is available from any single method alone.

Many new data on isotope shift measurements have been published in recent years; therefore, it is again the right moment to see another summary of facts and trends in the field. This is already done in the recent paper [7], which presents and discusses not only the isotopic trend of nuclear charge radii but also a full systematic of isotonic shifts extracted from the wealth of data. Special attention is paid to the structural evolution along the isotonic and isotopic chains around the “traditional” magic numbers 8, 20, 28, 50, 82 and 126 and to the appearance of new non-traditional magic numbers especially in the region of light nuclei. However, discussing the consequences of the R -tabulation, the paper [7] does not give numerical values of R ’s. The latter, together with short explanations, are accessible online in the database of the Lomonosov Moscow State University, Skobeltsyn Institute of Nuclear Physics and are presented as three different data sets (see Refs. [8–10]). A modified and updated version can be found in the site Data Library of NDS IAEA [11] as a single data set.

The purpose of this paper is to present in a compact form the numerical values of the experimental rms charge radii obtained by a combined treatment of the experimental data of both types – R and $\delta\langle r^2 \rangle$. The results of two different methods of data evaluation

[12,13] are combined into a single data set (Table 1). This is for the benefit of data users, who generally prefer a single, unified data set to several separate tables. Also a few new data are added, due to the last achievements of laser spectroscopy (see references to Table 2). Therefore, the resulting tabulation of radii covers a broader range of Z and N than most recently published tables [10,11]: it contains 909 isotopes for 92 elements.

2. Evaluation procedures

The principle of a combined treatment is obvious: a simple relation

$$R^2(A) = R^2(A') + \delta\langle r^2 \rangle^{A'A} \quad (1)$$

links the data on rms radii R ($R = \langle r^2 \rangle^{1/2}$) of a stable reference isotope A' with the radius change

$$\delta\langle r^2 \rangle^{A'A} = \langle r^2 \rangle^A - \langle r^2 \rangle^{A'} \quad (2)$$

between A' and a radioactive isotope A , giving the $R(A)$ value of any isotope A in a long isotopic sequence. The extraction of R according to this simple equation meets with serious statistical and computational problems in cases where there exist data on $R(A)$ for many isotopes and especially on $\delta\langle r^2 \rangle$ in long isotopic chains. So far three essentially different methods of combined analysis have been developed and the tabulated rms charge radii have been published [4,12–14]. Details of the different data treatments can be found in the original papers. Below only a brief description is given.

In Ref. [12] an algorithm is suggested for averaging the data for all known radii of isotopes and for all known chains of radii changes between isotopic pairs of the same element. It is a least square fit procedure in which the experimental data from electron scattering (e^-) and muonic atom X-rays (μ^-) are fitted to the more accurate radii changes in an isotopic sequence. Therefore, Ref. [12] lays stress on the ms radii changes and the resulting R values along long isotopic sequences correspond exactly to Eq. (1). The method has two disadvantages: (1) due to averaging over many different isotopic chains, it underestimated slightly the total uncertainties and (2) using the input data on $R_{e\mu}$ as given by [15], it doesn’t take into account any isotonic or isobaric $R_{e\mu}$ dependence.

On the contrary, in the evaluation procedure of Ref. [13], first R and δR values (also from non-isotopes) were taken into account from electron scattering (e^-), muonic atom X-rays (μ^-), K_α X-ray isotope shifts (KIS) and from optical isotope shifts along the valley of stability. Owing to the large number of independent and redundant R and δR data, weighted averaging and several constraints were applied resulting in a more accurate and consistent set of average $R_{e\mu KO}$ and $\delta R_{e\mu KO}$ data for stable nuclei. This data set can be regarded as a “backbone” for the next step. The uncertainty $\Delta\delta R_{e\mu KO}$ of the average differences $\delta R_{e\mu KO}$ is significantly less than that of the input data (e.g., it is less than the (total) error $\Delta\delta R_{OIS}$

of δR_{OIS}). The reduction of the total error from $\Delta\delta R_{OIS}$ to $\Delta\delta R_{e\mu KO}$ varied from element to element between 0.2 and 0.6. As δR values of a given isotopic series with n members are linearly interrelated with each other,

$$\delta R^{A',A_k} = \delta R^{A',A} \times \sqrt{\frac{\delta v_{FS}^{A',A_k}}{\delta v_{FS}^{A',A}}} \quad k = 1, 2, \dots, n-1 \quad (3)$$

correction factors $\delta R_{e\mu KO}/\delta R_{OIS}$ were formed; their values varied between 0.9 and 1.3 depending on the element. These factors were used to multiply those δR_{OIS} values of the isotopic chain, for which only OIS measurements were available, thus correcting for the common – Z -dependent – systematic errors. These corrected series of differences (“wings”) were added to the *backbone*. In this way a set of *rms* radii R was obtained. As the correction factor has the same value for a given element, this correction does not change the *relative* trend of $R_Z(N)$ isotopic dependence. However it improves the *absolute* R values, which are important for the investigation of the radius surface $R(N, Z)$ (e.g., for isotonic dependence). It is evident from the above that the δR_{OIS} values as obtained by OIS measurements, are not to be expected to fit exactly into the system of R data so derived. Thus, the algorithm [13] improves the links between different isotopic series, helping the study of isotonic and isobaric behaviour. This is its main advantage.

Fricke et al. [4,14] proposed a “model independent” way to determine parameters needed to extract radii changes from OIS using the so called King-plot [16]. This procedure essentially correlates OIS-data via King-plots with R , extracted from isotopic shift measurements in muonic atoms. Additional input enters from elastic electron scattering experiments wherever data are available; this concerns higher radial moments of the nuclear charge distribution. In the majority of cases the results from this model independent analysis agree passably with those obtained from electron shell data.

In all cases, the combined treatment is applicable to those elements for which both types of data, on R and $\delta\langle r^2 \rangle$, exist. The differences in the absolute R -values between these data sets are usually less than or around one percent. Although small, these differences lead to unexpected charge radii behavior in some cases of Ref. [14] which is not consistent with nuclear ground state properties. The problem is already discussed in Refs. [7,17]. On the contrary, the data sets of Refs. [8,9] are very close. Both data sets show the same fundamental properties and, what is of special importance, are consistent with gross nuclear radii trend and other nuclear ground state characteristics.

All the source data of Refs. [8,9] are carefully checked and even, when necessary, re-evaluated and updated. A careful analysis of the results has been performed, showing that the simple average values, R_{av} , of the two data sets can be regarded as “the best” experimental R tabulation. $R = R_{av}$ expresses in a great extent the advantages of both algorithms of combined analysis: improves the radii of stable nuclei replacing $R_{e\mu}$ by the more accurate $R_{e\mu KO}$ according to the algorithm of Ref. [13] and comprises the exact values of $\delta\langle r^2 \rangle$ according to the algorithm of Ref. [12]. The uncertainties $\Delta R_{tot} = \Delta\delta R_{e\mu KO, tot}$ of the *rms* radii R account for the total, statistical and systematic errors of both types of source data, as calculated by the method of Refs. [12,13]. To reflect the possible systematic discrepancies between two different evaluations we adopt a single unified set of uncertainties defined as

$$\Delta R_{tot} = \max(\Delta R [12], \Delta R [13], 0.5 \times |R [12] - R [13]|). \quad (4)$$

Only in 4% of all cases the differences between the two data sets of R are dominant. This is probably due to the statistical nature of data.

The new radii tabulation (Ref. [7] and the present work) permits to draw not only qualitative but also quantitative conclusions about the isotopic and isotonic radii trend for an extended range

of Z and N : $1 \leq Z \leq 96$ and $1 \leq N \leq 152$. Let us emphasize that both data sets [8,9] on which Table 1 is based are not a result of a simple compilation of individual measurements, but contains self-consistent set of R values giving a global survey of nuclear charge radii over the whole nuclide chart.

3. Data sources

3.1. Radii changes from optical isotope shift

In the algorithms of Refs. [12,13], the sources of data on nuclear parameters λ and $\delta\langle r^2 \rangle$ published before 1989 are the compilations Refs. [5,18]. Only a limited number of original papers after 1989 are used in Ref. [12], while the tables of Ref. [13] take into account a large amount of more recent results. The reference list to Table 2 of this work presents the updated data sources on $\delta\langle r^2 \rangle$. About 25% of the OIS data are published or found since the previous tables from 2004 covering 799 ground states. Compared to 2004 [13], and even compared to 2008 [10], many new data are added in the present table including information up to mid 2011. The radii changes in isotopic chains for He, Li, Be, Ne, Sc, Mn, Y, Nb, Ir, Bi are either first obtained or revised in the last years and, several isotopic sequences are recently extended to regions far off stability (e.g., Ar, Mo, Sn, Te, Pb, Po). In some cases (Ca, La, Eu, Gd, Hf) only single additional radioactive isotopes are added to the already existing data. In recent papers new results on *rms* charge radii are published based on OIS measurements: ^{74}Rb [19], $^{21-32}\text{Mg}$ [20], ^{12}Be [21] and $^{63-82}\text{Ga}$ [22].

Given the fact that the previous evaluation of $\delta\langle r^2 \rangle$ all over the nuclide chart [5] is already more than two decades old, we display in Table 1 also the source data on charge radii changes reflecting today's status in this research area. As many changes and improvements are included, we believe that the information on $\delta\langle r^2 \rangle$ may be of general usefulness to many researchers from experimental and theoretical point of view. The details about the choice of these data and on how the displayed $\delta\langle r^2 \rangle$ values have been derived are given in Table 2.

For extraction of nuclear radii changes from experimental OIS one needs to know two parameters, the so called electronic factor, F , related to the change in the electronic density at the nucleus for the optical transition and the mass shift constant, MS , accounting for the finite mass of the nucleus. The latter consists of two terms: normal, N , and specific, S , mass shift constants: $MS = N + S$. The procedure of extraction of nuclear radii changes from OIS is well known and described many times. For this reason, without going into details, we only present the equations which have been used for evaluation of $\delta\langle r^2 \rangle$.

The isotope shift, i.e. the difference in frequency

$$\delta\nu^{A',A} = \nu^A - \nu^{A'} \quad (5)$$

of a particular atomic transition between two isotopes with masses m_A and $m_{A'}$ can be decomposed into mass shift, $\delta\nu_{MS}$, arising from the change of the nuclear mass, and field shift $\delta\nu_{FS}$, sensitive to a change in the charge distribution inside the nucleus. It is caused by the additional neutrons and is proportional to the nuclear parameter λ :

$$\delta\nu^{A',A} = \delta\nu_{FS}^{A',A} + \delta\nu_{MS}^{A',A} = F\lambda^{A',A} + \frac{m_A - m_{A'}}{m_A m_{A'}}(N + S). \quad (6)$$

The nuclear parameter λ takes into account the change of the electronic wave function over the nuclear volume. This requires an expansion into a power series of the radial moments of the nuclear charge distribution [23]

$$\begin{aligned} \lambda^{A',A} &= \delta\langle r^2 \rangle^{A',A} + \sum \frac{C_k(Z)}{C_1(Z)} \delta\langle r^2 \rangle^{2k} \\ &= \delta\langle r^2 \rangle^{A',A} \left[1 + \sum_{k=1} \frac{C_k}{C_1} \delta\langle r^2 \rangle^{2k} / \delta\langle r^2 \rangle^{A',A} \right]. \end{aligned} \quad (7)$$

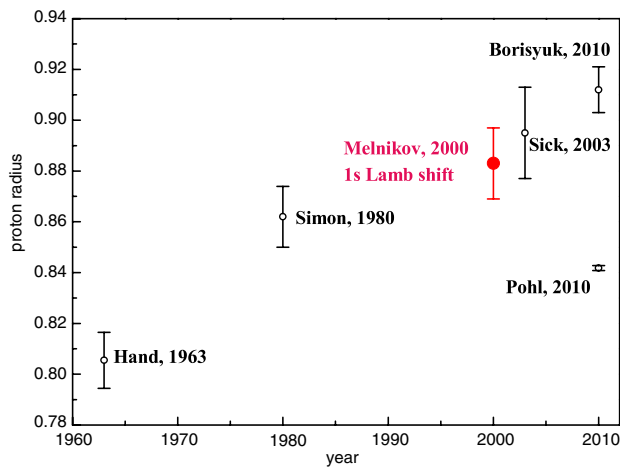


Fig. 1. Development of the experimental values of the proton radius during the years: Hand, 1963 [33], Simon, 1980 [34], Melnikov, 2000 [35], Sick, 2003 [36], Borisjuk, 2010 [37] and Pohl, 2010 [38].

For light nuclei, the contribution of higher order moments, the so called higher moments correction (HM), is vanishingly small, usually less than the experimental errors, and therefore $\lambda \approx \delta\langle r^2 \rangle$. For the heaviest nuclei the radial moments higher than $\delta\langle r^2 \rangle$ contribute almost 10%. A well developed procedure has been applied [13,14] to convert the experimental λ into $\delta\langle r^2 \rangle$. This is done for all isotopes with $Z \geq 36$.

Traditionally, F has been evaluated from atomic electron shell data using either semi-empirical procedures and/or Hartree–Fock methods for calculating the relevant electronic density at the site of the nucleus. The normal mass shift constant, given by $N = \nu m_e$, is calculated with the transition frequency ν and the electronic mass m_e . The specific mass shift constant, S , accounting for the correlations of the electronic motion, can be calculated reliably only for very light elements. In all cases of medium mass and heavy elements, different kinds of semi-empirical methods have been used. These methods of F and MS evaluation have yielded very consistent sets of $\delta\langle r^2 \rangle^{A',A}$ -values [5] all over the nuclear chart and even for very long isotopic chains. They didn't produce (e.g., unreasonable crossings of the isotopic course of nuclear radii between different elements). More importantly, the results could be interpreted in quantitative agreement with other well established experimental facts of nuclear structure. For extracting the nuclear parameter λ from OIS, the semi-empirical approach using optical information was preferred whenever possible (see Table 2 and the corresponding references).

When more than one data set on OIS is available, generally the most precise value that has been published was used. In many cases it was necessary to compile data from different sources and to reanalyze them.

3.2. Radii differences between isotopes from K_α isotope shifts

Most of the 89 K_α X-ray IS data are from Table II of Ref. [4], which is an extended version of Ref. [24]. Original papers have also been taken into account [25–27]. Two modifications were performed in Table II of Ref. [4]: (1) For uranium the correct mass interval is $^{233-238}\text{U}$ instead of $^{235-238}\text{U}$ (see Ref. [28]). (2) Regarding the results of a χ^2/ν test [29], the shift for $^{121-123}\text{Sb}$ [30] was omitted and some errors increased. In the table and papers referred above, energy shifts δE_{Coul} are given, which can be expressed in terms of even moments of the charge distribution: $\delta E_{\text{Coul}} = C_1 \lambda$, where the nuclear parameter λ contains the information on the size of the nucleus. Exploiting the wealth of δR data from e^- and μ^- experiments, it was possible to compare the theoretically

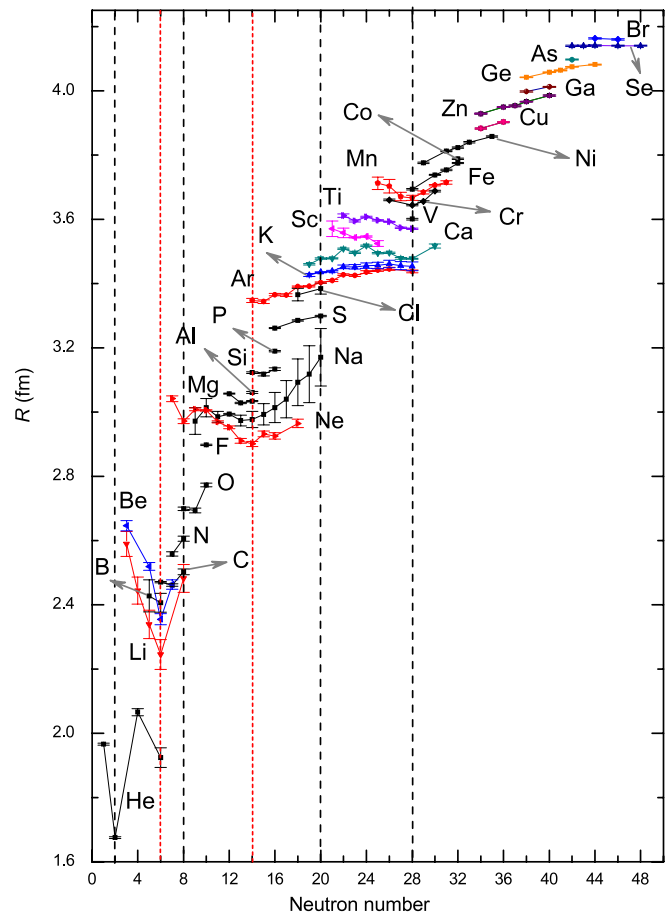


Fig. 2. Isotopic behaviour of rms charge radii for light elements from ^2He to ^{35}Br . For the sake of completeness the R -values obtained by non-optical methods are also shown. The error bars include the total, statistical and systematic uncertainties of the input data. The dashed vertical lines denote the conventional shell closures, while the small-dashed lines indicate the appearance of non-traditional magic numbers (see Ref. [7]).

calculated C_1 value to experiment in a wide range of atomic numbers, and to perform a small (0.965) correction on it. For more details see Section 2.5 of Ref. [13].

3.3. rms radii from e^- and μ^- experiments

The main source for the R values is the table of Ref. [15] which summarizes data from a large number of e^- and μ^- experiments, explains in detail the sources and selection of these data, as well as the statistical procedure of the combined treatment of both data types. Here we briefly mention only the changes. *Change in the evaluation:* for the absolute R data from e^- and μ^- methods, the simpler and more transparent averaging formulae were used (EXCEL) instead of the lengthy (FORTRAN) procedure (see Chapter 4 in Ref. [15]). This resulted in small changes in the mean R values. *New data:* for the stable isotopes of 9 elements, the table [15] contains rms radius values evaluated model independently by combining electron scattering, muonic atoms X-ray and optical isotope shifts. These are: Ca, Kr, Sr, Zr, Mo, Sn, Sm, Gd and Pb. In the first step of the present updated version of combined treatment, the R values for these isotopes are recalculated using only e^- and μ^- data sources and then, in a second step, two different procedures [12,13] of combined analysis with OIS data are performed. The radii of U and Th isotopes are also recalculated in view of critical remarks from Kozhedub [31].

Special attention deserves the new value for the radius of ^6Li obtained by analysis of electronic scattering experiments data and

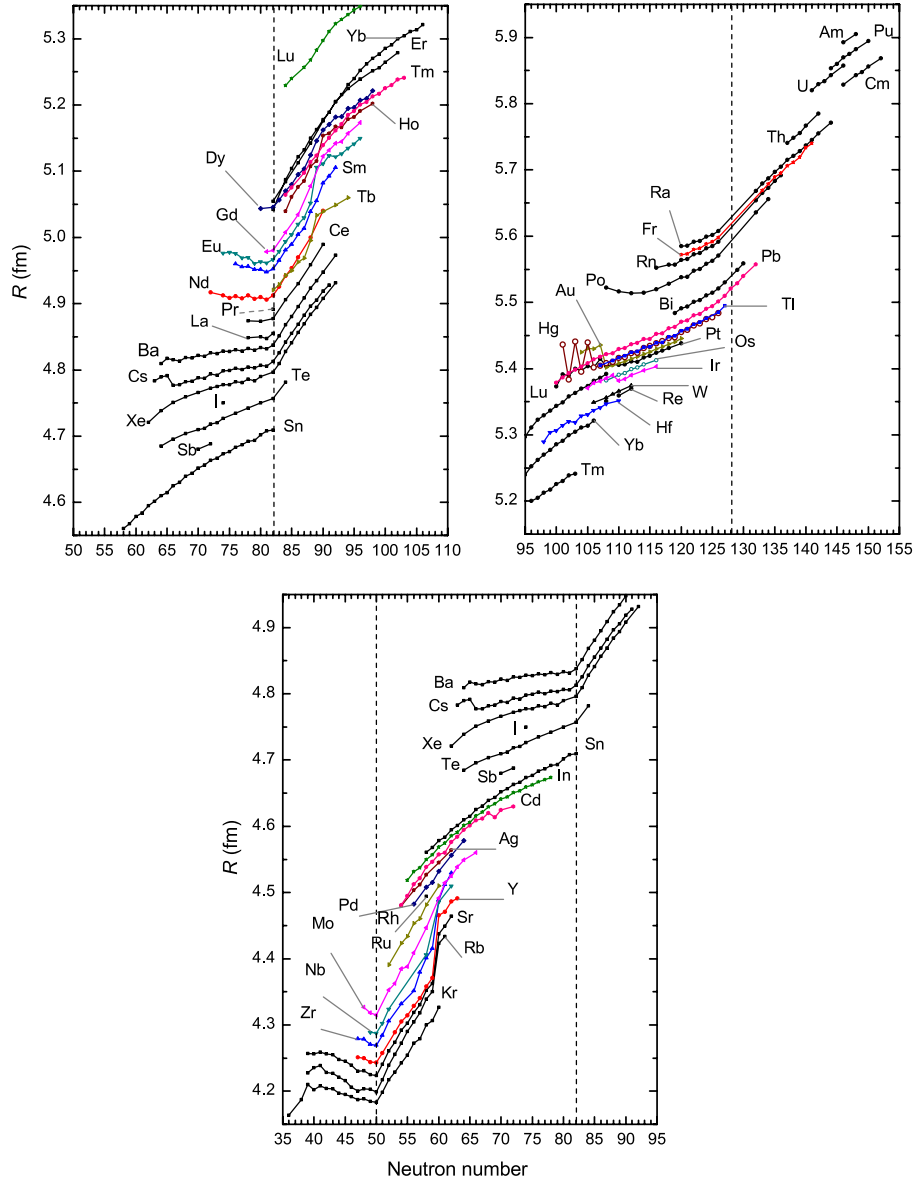


Fig. 3. Isotopic behaviour of *rms* charge radii for medium mass and heavy elements: from ^{36}Kr to ^{96}Cm . For clear presentation, these elements are grouped in three panels with identical *R* and *N* scales in such a way that the major neutron shell closures at $N = 50, 82$ and 126 are well pronounced.

theoretical calculations [32]. Nörtershäuser et al. [32] used this value as absolute reference for the radii in the Li isotopic chain and their results, the most correct existing data for Li, are displayed without any changes in Table 1.

Let us note that for Re, Po, Rn, Fr, Ra and Cm there are no experimental *R* data. Reference radii R_0 are calculated by the formula

$$R_0 = \left(r + \frac{r_1}{A_0^{2/3}} + \frac{r_2}{A_0^{4/3}} \right) \times A_0^{1/3} \quad (8)$$

with parameters: $r_0 = 0.9071(13)$ fm, $r_1 = 1.105(25)$ fm, $r_2 = -0.548(34)$ fm, which are the results of a least-squares fit to radii along the line of stability (see Table 2 in Ref. [13]). These parameters are correlated. Therefore for safety's sake, for the uncertainty ΔR_0 the value $2 \times (\Delta R_{0,\text{unc}})$ was used, where $\Delta R_{0,\text{unc}}$ is the value calculated by the assumption of uncorrelated parameters.

It is worth considering the problems connected with the proton radius the experimental value of which strongly changed during the years (see Fig. 1 and references therein [33–38]). In 2010, a

measurement of *muonic* hydrogen atom Lamb shift [38] resulted in an *rms* charge radius value $r_{p,\mu} = 0.84184(67)$ fm, which differs significantly from the earlier values obtained by electronic measurements (see e.g. 2nd paragraph in Section 2.1. of Ref. [13] and Section 5 in Ref. [7]). This strong deviation between electronic and muonic results may question the correctness of some quantum electrodynamics (QED) calculations or even the validity of the Standard Model of particle physics [39], and produced an active interest in the literature [40–44]. As this problem is not yet settled, it seems advisable to remain on the safe side, and to restrict ourselves to data derived from electronic measurements. See also [45].

4. Global behaviour of *rms* nuclear charge radii

Transforming $\delta\langle r^2 \rangle$ into absolute *rms* radii values, one receives a global overlook on the charge radii trend in an extended region of nuclei from He to Cm. The accuracy of the combined data is high compared to that of the directly measured radii values for the same element.

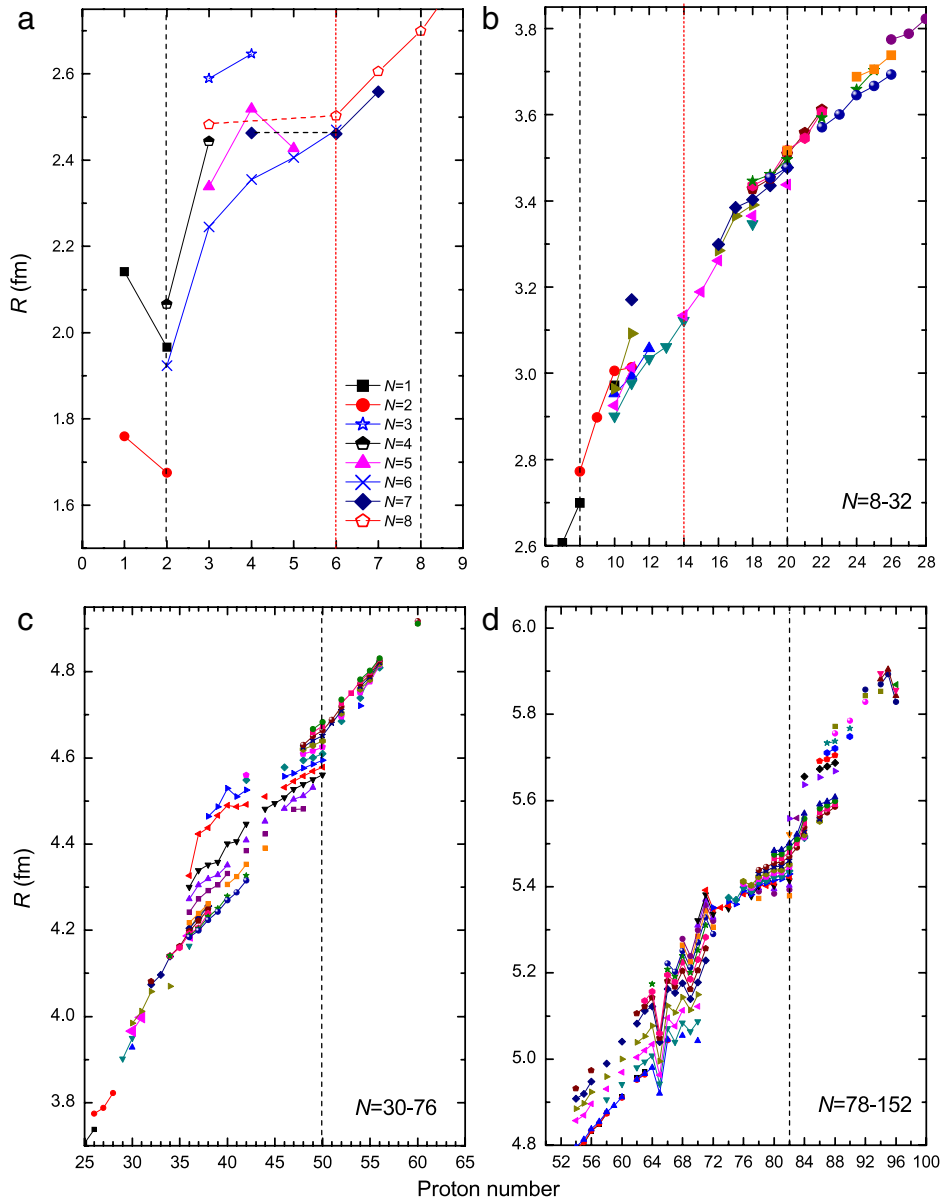


Fig. 4. Isotonic behaviour of *rms* radii *R* over the whole nuclide chart. In this case only the *R*-scales in all panels are identical. For visual simplicity only even *N* curves are drawn in panels (b)–(d). Special attention is paid to the region of light elements: panel (a), elements from ${}^1_1\text{H}$ to ${}^8_8\text{O}$ where isotonic curves for all odd and even *N*-values are drawn.

The dependences of the *rms* nuclear radii on neutron number *N* and proton number *Z* are demonstrated in Figs. 2–4. Adding new data to that of Ref. [10] does not influence the global features of the isotopic (Figs. 2 and 3) and the isotonic (Fig. 4a–d) radii developments. Different aspects of the nuclear radii tabulation can be considered. Those include (i) general features of the isotopic and isotonic trends; (ii) appearance of non-traditional magic numbers; (iii) new exotic phenomena that have been observed in the region of light nuclei; (iv) influence of the deformations; (v) data reliability, and (vi) comparison between theory and experiment. As all consequences of the radii tabulation are already discussed in detail in our previous work [7], here we summarize briefly only those which refer to the appearance or disappearance of magic numbers.

The conventional nucleon magic numbers 2, 28, 50 and 82 are evident from the charge radii development. The effect can be seen in Figs. 2–4 showing that the slope of the isotopic and isotonic curves is steeper at the beginning of an interval between two magic numbers and tends to saturate at the end. Therefore,

the shell closure effect on the charge radii manifests itself in characteristic slope changes (kinks) of radii at magic neutron and proton numbers. As has been shown in our previous work [7], a quantitative criterium of finding shell closure effects can be applied even if the eye is uncertain in deciding about its existence. This is the case for $N = 126$ and for most of the isotonic series.

New data in the region of light nuclei are of great importance, showing interesting peculiarities. Some of those are already discussed in Ref. [7]. For example, there is a strong indication that for nuclei with *Z* around 10, the neutron numbers $N = 6$ and $N = 14$ (or $N = 16$) may be magic or magic like instead of the conventional magic numbers $N = 8$ and $N = 20$ (see subsection 3.2 of Ref. [7]). From the point of view of isotopic nuclear radii behavior, the magic number $N = 20$ has no visible influence on the development of the charge radii in the case of stable nuclei in the Ca region (see Fig. 2). In the mass region $A = 100$, the double magicity of ${}^{96}\text{Zr}$ [46] is also confirmed by the *rms* charge radii trend [7].

Here we call the attention on Fig. 4a, where a characteristic slope change of the isotonic curve at $Z = 6$ for $N = 8$ and also

Table A

Comparison of $J^\pi = 2^+$ and 4^+ level energies, transition probabilities $B(E2)^\uparrow$ and the parameters of the quadrupole deformation in the isotonic series $N = 8$ confirming the double magicity of ^{14}C [48].

Element	Z	$E(2^+)$ (keV)	$E(4^+)/E(2^+)$	$B(E2)^\uparrow(e^2b^2)$	β_2
^{12}Be	4	2102	–	–	–
^{14}C	6	7012	1.53	0.00187	0.360(24)
^{16}O	8	6917	1.72	0.00406	0.364(17)
^{18}Ne	10	1887	1.79	0.0269	0.640(27)

for $N = 7$ appears. It corresponds to the closure of the proton $1p_{3/2}$ subshell and is in agreement with other ground state nuclear properties, signifying magicity of the (Z, N) pair $Z = 6, N = 8$ [47,48]. Table A illustrates some of them. The local maximum of the energy $E_1(2^+)$ of the first 2^+ excited state, the minimum of the ratio $E_1(4^+)/E_1(2^+)$ of the energies of the first $J^\pi = 4^+$ and $J^\pi = 2^+$ states and the minimum of $B(E2)^\uparrow$ transition probability at ^{14}C are even more pronounced than in the case of the classical double magic ^{16}O . The two isotones ^{14}C and ^{16}O has the same quadrupole deformation parameter β_2 smaller than β_2 for the neighbouring isotope ^{18}Ne . As can be seen from Table A and is already shown in our previous work [7] as well as by other authors (see, e.g., Refs. [6, 49]), nuclear charge radii as a function of neutron (or proton) number correlate with other experimental spectroscopic and mass observables. Up to now there are not many attempts for searching such correlations, but they “would be highly desirable in view of the need for reliable nuclear models” [6] involving nuclei far from stability. This would provide a new perspective to study the structural evolution of nuclear ground states with N and/or Z .

Not all conclusions in Ref. [7] are unambiguous. However this work, in a combination with the present nuclear radii tabulation, gives a ground for a more general nuclear physics discussion and is a challenge for further experiments. The data present the *status quo* of our knowledge about experimental radii values.

Acknowledgments

The authors are grateful to W. Nörtershäuser for providing data on Li charge radii before its publishing. Thanks are due to Yu. Gangrsky for the helpful suggestions.

References

- [1] R. Hofstadter, H.R. Fechter, J.A. McIntyre, Phys. Rev. 92 (1953) 978.
- [2] H. de Vries, C.W. de Jager, C. De Vries, At. Data Nucl. Data Tables 36 (1987) 495.
- [3] R. Engfer, H. Schnewly, J.L. Vuilleumier, H.K. Walter, A. Zehnder, At. Data Nucl. Data Tables 14 (1974) 409.
- [4] G. Fricke, C. Bernhardt, K. Heilig, L.A. Schaller, L. Schellenberg, E.B. Shera, C.W. de Jager, At. Data Nucl. Data Tables 60 (1995) 177.
- [5] E.W. Otten, in: D.A. Bromley (Ed.), Treatise on Heavy-Ion Science, 1989, pp. 517–638.
- [6] H.-J. Kluge, Hyperfine Interact. 196 (2010) 295.
- [7] I. Angeli, Yu.P. Gangrsky, K.P. Marinova, I.N. Boboshin, S.Yu. Komarov, B.S. Ishkhanov, V.V. Varlamov, J. Phys. G 36 (2009) 085102.
- [8] I. Angeli, Recommended values of nuclear charge radii, 2008, <http://cdfe.sinp.msu.ru/services/radchart/radhelp.html#rad>.
- [9] Yu. Gangrsky, K. Marinova, Nuclear charge radii, 2008, <http://cdfe.sinp.msu.ru/services/radchart/radhelp.html#rad>.
- [10] Database of the Lomonosov Moscow State University, Skobel'syn Institute of Nuclear Physics. <http://cdfe.sinp.msu.ru/services/radchart/radmain.html>.
- [11] I. Angeli, K. Marinova, Nuclear charge radii – 2010, A newsletter of the Nuclear Data Section (NDS) Issue No. 50, 2010, 3 <http://www.pub.iaea.org/MTCD/publications/PDF/Newsletters/ND-NL-50.pdf> (p. 3) (see also <http://www.nds.iaea.org/livechart/>).
- [12] E.G. Nadjakov, K.P. Marinova, Yu.P. Gangrsky, At. Data Nucl. Data Tables 56 (1994) 133.
- [13] I. Angeli, At. Data Nucl. Data Tables 87 (2004) 185.
- [14] G. Fricke, K. Heilig, Landolt-Börnstein: Num. Data and Funct. Relat. in Science and Tech., in: New Series, Group I: Elem. Part., Nuclei and Atoms, vol. 20, Springer Verlag, 2004, 324 pages.
- [15] I. Angeli, Table of nuclear root mean square charge radii, INDC(HUN)-033, IAEA Nuclear Data Section, Vienna, 1999.
- [16] W.H. King, Isotope Shift in Atomic Spectra, Plenum Press, New York, 1984.
- [17] J. Libert, B. Roussière, J. Sauvage, Nuclear Phys. A 786 (2007) 47.
- [18] P. Aufmuth, K. Heilig, A. Steudel, At. Data Nucl. Data Tables 87 (1987) 455.
- [19] E. Mané, et al., Phys. Rev. Lett. 107 (2011) 212502.
- [20] D.T. Yordanov, et al., Phys. Rev. Lett. 108 (2012) 042504.
- [21] A. Krieger, et al., Phys. Rev. Lett. 108 (2012) 142501.
- [22] T.J. Procter, et al., Phys. Rev. C 68 (2012) 034329.
- [23] E.C. Seltzer, Phys. Rev. 188 (1969) 1916.
- [24] F. Boehm, P.L. Lee, At. Data Nucl. Data Tables 14 (1974) 605.
- [25] P.L. Lee, F. Boehm, A.A. Hahn, Phys. Rev. C 17 (1978) 185.
- [26] C.W.E. Eijk, J. Wijnhorst, M.A. Popelier, W.A. Gillespie, J. Phys. G 5 (1979) 315.
- [27] S.R. Elliott, P. Beiersdorfer, M.H. Chen, Phys. Rev. Lett. 76 (1996) 1031.
- [28] R.T. Brockmeier, F. Boehm, E.N. Hatch, Phys. Rev. Lett. 15 (1965) 132.
- [29] I. Angeli, Hyperfine Interact. 136 (2001) 17.
- [30] A.S. Ryl'nikov, A.I. Egorov, G.A. Ivanov, V.I. Marushenko, A.F. Mezentssev, A.I. Smirnov, O.I. Sumbaev, V.V. Fyodorov, J. Exp. Theor. Phys. 63 (1972) 53.
- [31] Yu. Kozhedub, (St. Petersburg State University), private communication, 2007.
- [32] W. Nörtershäuser, T. Neff, R. Sánchez, I. Sick, Phys. Rev. C 84 (2011) 024307.
- [33] L.N. Hand, D.G. Miller, R. Wilson, Rev. Modern Phys. 35 (1963) 335.
- [34] G.G. Simon, Ch. Schmitt, F. Borkowski, V.H. Walther, Nuclear Phys. A 333 (1980) 381.
- [35] K. Melnikov, T. van Ritbergen, Phys. Rev. Lett. 84 (2000) 1673.
- [36] I. Sick, Phys. Lett. B 576 (2003) 62.
- [37] D. Borisyuk, Nuclear Phys. A 843 (2010) 59.
- [38] R. Pohl, A. Antognini, F. Nez, et al., Nature 466 (2010) 213.
- [39] J. Flowers, Nature 466 (2010) 195.
- [40] M.O. Distler, J.C. Bernauer, Th. Walcher, Phys. Lett. B 696 (2011) 343.
- [41] A. De Rujula, Phys. Lett. B 697 (2011) 26.
- [42] U.D. Jentschura, Ann. Phys. 326 (2011) 500.
- [43] U.D. Jentschura, Ann. Phys. 326 (2011) 516.
- [44] G.A. Miller, A.W. Thomas, J.D. Carroll, J. Rafelski, Natural resolution of the proton size puzzle. [arXiv:1101.4073v1](https://arxiv.org/abs/1101.4073v1) [physics.atom-ph] 21 Jan 2011.
- [45] J.C. Bernauer, et al., Phys. Rev. Lett. 105 (2010) 242001.
- [46] I.N. Boboshin, V.V. Varlamov, B.S. Ishkhanov, E.A. Romanovsky, Phys. Atomic Nuclei 70 (2007) 1363.
- [47] B.A. Brown, W.A. Richter, Phys. Rev. C 72 (2005) 057301.
- [48] O. Sorlin, M.-G. Porquet, Prog. Part. Nucl. Phys. 61 (2008) 602.
- [49] R.B. Cakirli, R.F. Casten, K. Blaum, Phys. Rev. C 82 (2010) 061306(R).
- [50] W. Nörtershäuser, Hyperfine Interact. 198 (2010) 73.

Explanation of Tables

Table 1.	Nuclear radii changes and <i>rms</i> nuclear charge radii. (The IS and charge radii changes in the isotopic sequence $^{21-32}\text{Mg}$ are already measured by the Mainz-COLLAPS collaboration (see Ref. [50]) but are as yet not published. For this reason Table 1 include only <i>R</i> -values of stable Mg isotopes as given in Ref. [15].)
<i>Z</i>	Atomic (proton) number of the element
<i>El</i>	Chemical symbol of the element
<i>A</i>	Mass number
<i>N</i>	Neutron number
$\delta\langle r^2 \rangle^{A',A}$	Nuclear radii changes from OIS (column 5). $\delta\langle r^2 \rangle^{A',A} = \lambda^{A',A}$ for $Z \leq 35$; in all cases with $Z \geq 36$ the higher moment (HM) corrections have been taken into account. This is done either by the authors themselves or recalculated using the average values of HM as given by Ref. [14].
$\Delta\delta\langle r^2 \rangle^{A',A}$	Errors of radius changes (column 6). Only statistical errors are presented thus demonstrating the accuracy of optical isotope shift measurements. Some exceptions are explicitly pointed in Table 2.
<i>R</i>	The average <i>rms</i> $R = R_{e\mu KO}$ -values of both procedures of combined analysis [12,13] (column 7). Note that the experimental bases and evaluation procedures underlying these <i>R</i> values are not identical with those for $\delta\langle r^2 \rangle^{A,A'}$; see Chapter 2.
$\Delta_{tot}R$	The total errors of <i>R</i> (column 8) defined by Eq. (4). It includes the uncertainties ΔR of absolute radii, statistical and systematic errors of $\delta\langle r^2 \rangle$ as obtained by the evaluation procedure of Ref. [13] and the deviation between the results of the two procedures (see Section 2). In the case if the latter are dominant, these errors are underlined.
$\Delta_{rel}R$	Relative error of $R_{e\mu KO}$ with respect to the reference isotope for radii changes (Column 9).

Table 2.	Parameters used for extraction of radii changes from OIS
	<i>Note:</i> References given by number are from the reference list to the main text; references given by abbreviations of name and year are from the reference list to Table 2.
<i>F</i>	Electronic factor
<i>N</i>	Normal mass shift
<i>S</i>	Specific mass shift
<i>MS</i>	Mass shift, where $MS = N + S$
	Abbreviation related to the electronic factor <i>F</i> and the total mass shift <i>MS</i>
<i>cal</i>	Atomic theory calculation; for the theoretical method used (see the corresponding papers)
<i>se</i>	Semi-empirical procedure using optical data (e.g., Ref. [5])
$e^-, \mu^-, e\mu$	Calculated via King plot [16] of OIS versus e^-, μ^- or $e\mu$ radii
<i>phen</i>	Estimated using $\delta\langle r^2 \rangle^{N',N}$ of neighboring isotones.
	Errors of <i>F</i> and <i>MS</i>
dF_{cal}, dMS_{cal}	Accepted 10% if not theoretically estimated
dF_{se}	Between 1% [BI85, table reference] and 10% (in most cases)
dMS_{se}	For medium mass and heavy elements [He74], where $dMS_{se} = 0.5N$ for s^2 -sp transitions with $S = (0 \pm 0.5)N$, $dMS_{se} = 0.9N$ for s-p transitions with $S = (0.3 \pm 0.9)N$
$dF_{e\mu}, dMS_{e\mu}$	Obtained in the least square fit procedure of King plot.
dF_{phen}, dMS_{phen}	Estimations.

Table 1Nuclear radii changes and *rms* nuclear charge radii. For the neutron the entry is $\langle r^2 \rangle$ (fm²).

Z	el.	A	N	$\delta\langle r^2 \rangle$ (fm ²)	$\Delta\delta\langle r^2 \rangle$ (fm ²)	R (fm)	$\Delta_{\text{tot}}R$ (fm)	ΔR_{rel}
0	n	1	1			−0.1149	0.0027	
1	H	1	0	0	0	0.8783	0.0086	
		2	1	3.82007	0.00065	2.1421	0.0088	
		3	2			1.7591	0.0363	
2	He	3	1	1.059	0.003	1.9661	0.0030	0.0008
		4	2	0	0	1.6755	0.0028	0
		6	4	1.466	0.034	2.0660	0.0111	0.0082
		8	6	0.911	0.095	1.9239	0.0306	0.0247
3	Li	6	3	0	0	2.5890	0.0390	0
		7	4	−0.731	0.022	2.4440	0.0420	0.0046
		8	5	−1.230	0.032	2.3390	0.0440	0.0070
		9	6	−1.663	0.032	2.2450	0.0460	0.0073
		11	8	−0.543	0.069	2.4820	0.0430	0.0141
4	Be	7	3	0.66	0.05	2.6460	0.0160	0.0094
		9	5	0	0	2.5190	0.0120	0
		10	6	−0.79	0.08	2.3550	0.0170	0.0170
		11	7	−0.28	0.05	2.4630	0.0150	0.0102
5	B	10	5			2.4277	0.0499	
		11	6			2.4060	0.0294	
6	C	12	6			2.4702	0.0022	
		13	7			2.4614	0.0034	
		14	8			2.5025	0.0087	
7	N	14	7			2.5582	0.0070	
		15	8			2.6058	0.0080	
8	O	16	8			2.6991	0.0052	
		17	9			2.6932	0.0075	
		18	10			2.7726	0.0056	
9	F	19	10			2.8976	0.0025	
10	Ne	17	7	0.221	0.029	3.0413	0.0088	0.0048
		18	8	−0.207	0.015	2.9714	0.0076	0.0025
		19	9	0.017	0.019	3.0082	0.0040	0.0032
		20	10	0	0	3.0055	0.0021	0
		21	11	−0.217	0.014	2.9695	0.0033	0.0023
		22	12	−0.322	0.004	2.9525	0.0040	0.0034
		23	13	−0.572	0.034	2.9104	0.0071	0.0057
		24	14	−0.628	0.019	2.9007	0.0078	0.0032
		25	15	−0.431	0.016	2.9316	0.0088	0.0027
		26	16	−0.485	0.018	2.9251	0.0100	0.0030
		28	18	−0.241	0.035	2.9642	0.0134	0.0059
11	Na	20	9	−0.130	0.070	2.9718	0.0420	0.0117
		21	10	0.120	0.050	3.0136	0.0284	0.0083
		22	11	−0.050	0.040	2.9852	0.0169	0.0067
		23	12	0	0	2.9936	0.0021	0
		24	13	−0.120	0.040	2.9735	0.0169	0.0067
		25	14	−0.100	0.030	2.9769	0.0252	0.0050
		26	15	−0.005	0.018	2.9928	0.0331	0.0030
		27	16	0.120	0.040	3.0136	0.0467	0.0067
		28	17	0.280	0.050	3.0400	0.0581	0.0083
		29	18	0.600	0.080	3.0922	0.0723	0.0132
		30	19	0.760	0.120	3.1180	0.0884	0.0197
		31	20	1.090	0.070	3.1704	0.0893	0.0116
12	Mg	24	12			3.0570	0.0016	
		25	13			3.0284	0.0022	
		26	14			3.0337	0.0018	
13	Al	27	14			3.0610	0.0031	
14	Si	28	14			3.1224	0.0024	
		29	15			3.1176	0.0052	
		30	16			3.1336	0.0040	
15	P	31	16			3.1889	0.0019	
16	S	32	16			3.2611	0.0018	
		34	18			3.2847	0.0021	
		36	20			3.2985	0.0024	
17	Cl	35	18			3.3654	0.0191	
		37	20			3.3840	0.0170	
18	Ar	32	14	−0.375	0.038	3.3468	0.0062	0.0056
		33	15	−0.395	0.021	3.3438	0.0058	0.0031
		34	16	−0.251	0.006	3.3654	0.0040	0.0009

(continued on next page)

Table 1 (continued)

Z	el.	A	N	$\delta\langle r^2 \rangle$ (fm ²)	$\Delta\delta\langle r^2 \rangle$ (fm ²)	R (fm)	$\Delta_{\text{rot}} R$ (fm)	ΔR_{rel}
19	K	35	17	−0.263	0.026	3.3636	0.0042	0.0038
		36	18	−0.084	0.018	3.3905	0.0023	0.0017
		37	19	−0.081	0.009	3.3908	0.0022	0.0012
		38	20	0	0	3.4028	0.0019	0
		39	21	0.044	0.067	3.4093	0.0031	0.0025
		40	22	0.167	0.009	3.4274	0.0026	0.0013
		41	23	0.151	0.012	3.4251	0.0030	0.0018
		43	25	0.262	0.012	3.4414	0.0041	0.0018
		42	24	0.221	0.014	3.4354	0.0039	0.0020
		44	26	0.289	0.009	3.4454	0.0046	0.0013
		46	28	0.237	0.022	3.4377	0.0044	0.0032
		38	19	−0.058	0.041	3.4264	0.0051	0.0060
		39	20	0	0	3.4349	0.0019	0
		40	21	0.022	0.002	3.4381	0.0028	0.0003
		41	22	0.117	0.006	3.4518	0.0055	0.0009
		42	23	0.116	0.015	3.4517	0.0070	0.0022
20	Ca	43	24	0.143	0.009	3.4556	0.0086	0.0013
		44	25	0.148	0.011	3.4563	0.0101	0.0016
		45	26	0.176	0.013	3.4605	0.0118	0.0019
		46	27	0.143	0.012	3.4558	0.0126	0.0017
		47	28	0.126	0.013	3.4534	0.0138	0.0019
		39	19	−0.127	0.016	3.4595	0.0025	0.0023
		40	20	0	0	3.4776	0.0019	0
		41	21	0.003	0.003	3.4780	0.0019	0.0004
		42	22	0.215	0.005	3.5081	0.0021	0.0007
		43	23	0.125	0.003	3.4954	0.0019	0.0005
21	Sc	44	24	0.283	0.006	3.5179	0.0021	0.0009
		45	25	0.119	0.006	3.4944	0.0021	0.0008
		46	26	0.124	0.005	3.4953	0.0020	0.0007
		47	27	0.005	0.001	3.4783	0.0024	0.0002
		48	28	−0.004	0.006	3.4771	0.0020	0.0009
		50	30	0.276	0.035	3.5168	0.0064	0.0050
		42	21	0.172	0.031	3.5702	0.0238	0.0044
		43	22	0.082	0.014	3.5575	0.0147	0.0020
22	Ti	44	23	−0.019	0.011	3.5432	0.0016	0.0016
		45	24	0	0	3.5459	0.0025	0
		46	25	−0.154	0.008	3.5243	0.0089	0.0011
		44	22	0.143	0.037	3.6115	0.0051	0.0049
		45	23	0.013	0.017	3.5939	0.0032	0.0024
		46	24	0.110	0.007	3.6070	0.0022	0.0010
23	V	47	25	0.030	0.004	3.5962	0.0019	0.0006
		48	26	0	0	3.5921	0.0017	0
		49	27	−0.139	0.009	3.5733	0.0021	0.0013
		50	28	−0.160	0.007	3.5704	0.0022	0.0010
		51	28			3.6002	0.0022	
24	Cr	50	26	0.099	0.037	3.6588	0.0065	0.0051
		52	28	0	0	3.6452	0.0042	0
		53	29	0.043	0.045	3.6511	0.0075	0.0062
		54	30	0.317	0.045	3.6885	0.0074	0.0061
25	Mn	50	25	0.046	0.003	3.7120	0.0196	0.0004
		51	26	−0.023	0.045	3.7026	0.0212	0.0061
		52	27	−0.259	0.013	3.6706	0.0128	0.0018
		53	28	−0.292	0.004	3.6662	0.0076	0.0005
		54	29	−0.165	0.007	3.6834	0.0049	0.0009
		55	30	0	0	3.7057	0.0022	0
		56	31	0.066	0.010	3.7146	0.0052	0.0013
26	Fe	54	28	−0.330	0.001	3.6933	0.0019	0.0001
		56	30	0	0	3.7377	0.0016	0
		57	31	0.108	0.001	3.7532	0.0017	0.0001
		58	32	0.274	0.002	3.7745	0.0014	0.0003
27	Co	59	32			3.7875	0.0021	
28	Ni	58	30	−0.267	0.005	3.7757	0.0020	0.0007
		60	32	0	0	3.8118	0.0016	0
		61	33	0.082	0.007	3.8225	0.0019	0.0010
		62	34	0.211	0.007	3.8399	0.0021	0.0009
		64	36	0.338	0.010	3.8572	0.0023	0.0013
29	Cu	63	34			3.8823	0.0015	
		65	36			3.9022	0.0014	
30	Zn	64	34	−0.162	0.002	3.9283	0.0015	0.0003
		66	36	0	0	3.9491	0.0014	0
		67	37	0.032	0.003	3.9530	0.0027	0.0004

(continued on next page)

Table 1 (continued)

Z	el.	A	N	$\delta(r^2)$ (fm ²)	$\Delta\delta(r^2)$ (fm ²)	R (fm)	$\Delta_{\text{tot}}R$ (fm)	ΔR_{rel}
31	Ga	68	38	0.131	0.002	3.9658	0.0014	0.0003
		70	40	0.286	0.003	3.9845	0.0019	0.0004
		69	38			3.9973	0.0017	
		71	40			4.0118	0.0018	
32	Ge	70	38			4.0414	0.0012	
		72	40			4.0576	0.0013	
		73	41			4.0632	0.0014	
		74	42			4.0742	0.0012	
		76	44			4.0811	0.0012	
33	As	75	42			4.0968	0.0020	
34	Se	74	40			4.0700	0.0200	
		76	42			4.1395	0.0016	
		77	43			4.1395	0.0018	
		78	44			4.1406	0.0017	
		80	46			4.1400	0.0018	
35	Br	82	48			4.1400	0.0019	
		79	44			4.1629	0.0021	
		81	46			4.1599	0.0021	
36	Kr	72	36	−0.168	0.018	4.1635	0.0060	0.0022
		74	38	0.030	0.005	4.1870	0.0041	0.0006
		75	39	0.221	0.007	4.2097	0.0041	0.0008
		76	40	0.156	0.004	4.2020	0.0036	0.0005
		77	41	0.209	0.005	4.2082	0.0037	0.0006
		78	42	0.172	0.003	4.2038	0.0033	0.0004
		79	43	0.168	0.004	4.2034	0.0032	0.0005
		80	44	0.114	0.007	4.1970	0.0029	0.0008
		81	45	0.099	0.004	4.1952	0.0026	0.0005
		82	46	0.071	0.003	4.1919	0.0025	0.0004
		83	47	0.031	0.003	4.1871	0.0023	0.0004
		84	48	0.042	0.001	4.1884	0.0022	0.0001
		85	49	0.009	0.004	4.1846	0.0022	0.0004
		86	50	0	0	4.1835	0.0021	0
		87	51	0.125	0.003	4.1984	0.0027	0.0004
		88	52	0.282	0.004	4.2171	0.0043	0.0005
		89	53	0.379	0.004	4.2286	0.0054	0.0005
		90	54	0.495	0.010	4.2423	0.0069	0.0012
		91	55	0.597	0.006	4.2543	0.0081	0.0007
		92	56	0.751	0.005	4.2724	0.0099	0.0006
		93	57	0.811	0.004	4.2794	0.0107	0.0005
		94	58	0.989	0.004	4.3002	0.0129	0.0005
		95	59	1.045	0.003	4.3067	0.0136	0.0004
		96	60	1.217	0.010	4.3267	0.0158	0.0012
37	Rb	76	39	0.2241	0.0270	4.2273	0.0070	0.0032
		77	40	0.2884	0.0069	4.2356	0.0080	0.0008
		78	41	0.3118	0.0023	4.2385	0.0083	0.0004
		79	42	0.2291	0.0023	4.2284	0.0065	0.0003
		80	43	0.2207	0.0068	4.2271	0.0061	0.0008
		81	44	0.1730	0.0022	4.2213	0.0051	0.0003
		82	45	0.1347	0.0065	4.2160	0.0042	0.0008
		83	46	0.0522	0.0015	4.2058	0.0028	0.0002
		84	47	0.0079	0.0032	4.1999	0.0023	0.0004
		85	48	0.0362	0.0022	4.2036	0.0024	0.0003
		86	49	0.0276	0.0031	4.2025	0.0023	0.0004
		87	50	0	0	4.1989	0.0021	0
		88	51	0.1390	0.0078	4.2170	0.0038	0.0010
		89	52	0.3109	0.0031	4.2391	0.0074	0.0004
		90	53	0.4370	0.0080	4.2554	0.0102	0.0010
		91	54	0.5685	0.0035	4.2723	0.0131	0.0007
		92	55	0.7094	0.0080	4.2903	0.0163	0.0010
		93	56	0.9340	0.0035	4.3048	0.0187	0.0010
		94	57	1.0984	0.0056	4.3184	0.0211	0.0011
		95	58	1.1856	0.0074	4.3391	0.0248	0.0014
38	Sr	96	59	1.7719	0.0062	4.3501	0.0267	0.0015
		97	60	1.8553	0.0150	4.4231	0.0395	0.0023
		98	61	1.8553	0.0150	4.4336	0.0414	0.0024
		77	39	0.253	0.012	4.2569	0.0044	0.0014
		78	40	0.247	0.008	4.2561	0.0040	0.0009
		79	41	0.266	0.006	4.2586	0.0039	0.0007
		80	42	0.248	0.007	4.2562	0.0037	0.0008
		81	43	0.236	0.006	4.2547	0.0034	0.0007
		82	44	0.182	0.006	4.2478	0.0030	0.0007
		83	45	0.165	0.004	4.2455	0.0027	0.0005

(continued on next page)

Table 1 (continued)

Z	el.	A	N	$\delta\langle r^2 \rangle$ (fm ²)	$\Delta\delta\langle r^2 \rangle$ (fm ²)	R (fm)	$\Delta_{\text{tot}} R$ (fm)	ΔR_{rel}
		84	46	0.118	0.003	4.2394	0.0024	0.0004
		85	47	0.049	0.003	4.2304	0.0021	0.0004
		86	48	0.051	0.002	4.2307	0.0020	0.0002
		87	49	0.007	0.002	4.2249	0.0019	0.0002
		88	50	0	0	4.2240	0.0018	0
		89	51	0.126	0.001	4.2407	0.0023	0.0001
		90	52	0.282	0.004	4.2611	0.0037	0.0005
		91	53	0.381	0.003	4.2740	0.0046	0.0004
		92	54	0.522	0.005	4.2924	<u>0.0064</u>	0.0006
		93	55	0.601	0.004	4.3026	<u>0.0075</u>	0.0005
		94	56	0.728	0.006	4.3191	<u>0.0091</u>	0.0007
		95	57	0.817	0.005	4.3305	<u>0.0102</u>	0.0006
		96	58	0.986	0.006	4.3522	<u>0.0125</u>	0.0007
		97	59	1.067	0.007	4.3625	<u>0.0135</u>	0.0009
		98	60	1.656	0.006	4.4377	<u>0.0214</u>	0.0008
		99	61	1.750	0.008	4.4495	<u>0.0226</u>	0.0011
		100	62	1.867	0.015	4.4640	<u>0.0240</u>	0.0019
39	Y	86	47	0.071	0.003	4.2513	0.0023	0.0008
		87	48	0.058	0.002	4.2498	0.0022	0.0007
		88	49	0.009	0.001	4.2441	0.0021	0.0001
		89	50	0	0	4.2430	0.0021	0
		90	51	0.123	0.001	4.2573	0.0026	0.0014
		92	53	0.393	0.001	4.2887	0.0050	0.0045
		93	54	0.537	0.002	4.3052	0.0065	0.0061
		94	55	0.614	0.001	4.3142	0.0074	0.0070
		95	56	0.738	0.002	4.3284	0.0087	0.0083
		96	57	0.840	0.001	4.3402	0.0099	0.0095
		97	58	0.996	0.002	4.3580	0.0116	0.0112
		98	59	1.110	0.001	4.3711	0.0129	0.0124
40	Zr	99	60	1.943	0.001	4.4658	0.0223	0.0213
		100	61	1.985	0.001	4.4705	0.0228	0.0218
		101	62	2.127	0.001	4.4863	0.0244	0.0232
		102	63	2.173	0.002	4.4911	0.0249	0.0237
		87	47	0.059	0.005	4.2789	0.0030	0.0006
		88	48	0.061	0.005	4.2787	0.0025	0.0006
		89	49	0.006	0.005	4.2706	0.0010	0.0006
		90	50	0	0	4.2694	0.0010	0
		91	51	0.132	0.003	4.2845	0.0013	0.0011
		92	52	0.314	0.004	4.3057	0.0013	0.0025
		94	54	0.546	0.003	4.3320	0.0013	0.0032
		96	56	0.72	0.006	4.3512	0.0015	0.0034
41	Nb	97	57	0.835	0.005	4.3792	<u>0.0136</u>	0.0006
		98	58	1.002	0.005	4.4012	<u>0.0164</u>	0.0006
		99	59	1.113	0.004	4.4156	<u>0.0181</u>	0.0006
		100	60	1.669	0.004	4.4891	<u>0.0289</u>	0.0006
		101	61	1.847	0.005	4.5119	<u>0.0318</u>	0.0007
		102	62	1.983	0.005	4.5292	<u>0.0340</u>	0.0008
		90	49	−0.301	0.004	4.2891	0.0040	0.0004
		91	50	−0.312	0.001	4.2878	0.0040	0.0001
		92	51	−0.185	0.002	4.3026	0.0043	0.0003
		93	52	0	0	4.3240	0.0017	0
		99	58	0.716	0.009	4.4062	0.0125	0.0010
		101	60	1.419	0.002	4.4861	0.0203	0.0002
42	Mo	103	62	1.630	0.002	4.5097	0.0227	0.0002
		90	48	0.113	0.001	4.3265	0.0016	0.0001
		91	49	0.033	0.002	4.3182	0.0012	0.0001
		92	50	0	0	4.3151	0.0012	0
		94	52	0.334	0.001	4.3529	0.0013	0.0001
		95	53	0.421	0.001	4.3628	0.0018	0.0001
		96	54	0.617	0.001	4.3847	0.0015	0.0001
		97	55	0.644	0.001	4.3880	0.0015	0.0001
		98	56	0.834	0.001	4.4091	0.0018	0.0001
		100	58	1.177	0.001	4.4468	0.0025	0.0001
		102	60	1.585	0.003	4.4914	0.0038	0.0001
		103	61	1.798	0.003	4.5145	0.0046	0.0002
44	Ru	104	62	1.893	0.002	4.5249	0.0051	0.0002
		105	63	2.021	0.003	4.5389	0.0057	0.0003
		106	64	2.113	0.003	4.5490	0.0058	0.0003
		108	66	2.213	0.003	4.5602	0.0067	0.0003
		96	52	−1.069	0.003	4.3908	0.0047	0.0003
		98	54	−0.772	0.005	4.4229	0.0055	0.0005
		99	55	−0.68	0.004	4.4338	0.0042	0.0004
		100	56	−0.506	0.003	4.4531	0.0031	0.0004

(continued on next page)

Table 1 (continued)

Z	el.	A	N	$\delta(r^2)$ (fm ²)	$\Delta\delta(r^2)$ (fm ²)	R (fm)	$\Delta_{tot}R$ (fm)	ΔR_{rel}
		101	57	−0.444	0.005	4.4606	0.0020	0.0006
		102	58	−0.263	0.004	4.4809	0.0018	0.0005
		104	60	0	0	4.5098	0.0020	0
45	Rh	103	58			4.4945	0.0023	
46	Pd	102	56	−0.675	0.003	4.4827	0.0044	0.0003
		104	58	−0.445	0.002	4.5078	0.0027	0.0002
		105	59	−0.377	0.002	4.5150	0.0030	0.0002
		106	60	−0.227	0.001	4.5318	0.0029	0.0001
		108	62	0	0	4.5563	0.0027	0
		110	64	0.205	0.001	4.5782	0.0030	0.0001
47	Ag	101	54	−0.670	0.003	4.4799	0.0088	0.0003
		103	56	−0.482	0.002	4.5036	0.0065	0.0002
		104	57	−0.416	0.002	4.5119	0.0058	0.0002
		105	58	−0.296	0.002	4.5269	0.0045	0.0002
		107	60	−0.148	0.001	4.5454	0.0031	0.0001
		109	62	0	0	4.5638	0.0025	0
48	Cd	102	54	−1.010	0.045	4.4810	<u>0.0122</u>	0.0050
		103	55	−0.901	0.027	4.4951	<u>0.0105</u>	0.0030
		104	56	−0.765	0.048	4.5122	<u>0.0083</u>	0.0053
		105	57	−0.692	0.034	4.5216	<u>0.0070</u>	0.0038
		106	58	−0.576	0.008	4.5383	0.0036	0.0009
		107	59	−0.495	0.030	4.5466	0.0039	0.0033
		108	60	−0.412	0.011	4.5577	0.0031	0.0012
		109	61	−0.387	0.039	4.5601	0.0035	0.0043
		110	62	−0.252	0.005	4.5765	0.0026	0.0005
		111	63	−0.130	0.013	4.5845	<u>0.0058</u>	0.0014
		112	64	−0.103	0.003	4.5944	0.0024	0.0003
		113	65	−0.008	0.004	4.6012	<u>0.0028</u>	0.0004
		114	66	0	0	4.6087	0.0023	0
		115	67	0.024	0.046	4.6114	<u>0.0046</u>	0.0050
		116	68	0.088	0.003	4.6203	<u>0.0059</u>	0.0003
		117	69	0.083	0.018	4.6136	0.0025	0.0020
		118	70	0.129	0.022	4.6246	<u>0.0060</u>	0.0024
		120	72	0.174	0.043	4.6300	<u>0.0069</u>	0.0046
49	In	104	55	−0.866	0.015	4.5184	0.0117	0.0017
		105	56	−0.754	0.014	4.5311	0.0103	0.0015
		106	57	−0.698	0.012	4.5375	0.0095	0.0013
		107	58	−0.592	0.010	4.5494	0.0082	0.0011
		108	59	−0.524	0.005	4.5571	0.0071	0.0006
		109	60	−0.422	0.007	4.5685	0.0061	0.0008
		110	61	−0.371	0.008	4.5742	0.0056	0.0009
		111	62	−0.270	0.005	4.5856	0.0044	0.0005
		112	63	−0.224	0.006	4.5907	0.0041	0.0007
		113	64	−0.1317	0.0003	4.6010	0.0031	0.0001
		114	65	−0.090	0.002	4.6056	0.0029	0.0002
		115	66	0	0	4.6156	0.0026	0
		116	67	0.049	0.001	4.6211	0.0027	0.0001
		117	68	0.122	0.004	4.6292	0.0032	0.0004
		118	69	0.162	0.002	4.6335	0.0033	0.0002
		119	70	0.226	0.004	4.6407	0.0040	0.0004
		120	71	0.259	0.002	4.6443	0.0042	0.0002
		121	72	0.315	0.003	4.6505	0.0047	0.0003
		122	73	0.342	0.004	4.6534	0.0051	0.0004
		123	74	0.396	0.003	4.6594	0.0056	0.0003
		124	75	0.424	0.004	4.6625	0.0060	0.0007
		125	76	0.465	0.005	4.6670	0.0064	0.0005
		126	77	0.494	0.007	4.6702	0.0068	0.0008
		127	78	0.523	0.007	4.6733	0.0071	0.0008
50	Sn	108	58	−0.825	0.003	4.5605	0.0029	0.0003
		109	59	−0.764	0.006	4.5679	0.0027	0.0007
		110	60	−0.666	0.002	4.5785	0.0025	0.0002
		111	61	−0.612	0.005	4.5836	0.0024	0.0005
		112	62	−0.520	0.005	4.5948	0.0022	0.0005
		113	63	−0.458	0.001	4.6015	0.0021	0.0001
		114	64	−0.3838	0.0001	4.6099	0.0020	0.0001
		115	65	−0.3360	0.0001	4.6148	0.0019	0.0001
		116	66	−0.2471	0.0001	4.6250	0.0019	0.0001
		117	67	−0.1971	0.0001	4.6302	0.0019	0.0001
		118	68	−0.1174	0.0001	4.6393	0.0019	0.0001
		119	69	−0.0724	0.0001	4.6438	0.0020	0.0001
		120	70	0	0	4.6519	0.0021	0
		121	71	0.045	0.001	4.6566	0.0021	0.0001
		122	72	0.1055	0.0001	4.6634	0.0022	0.0001

(continued on next page)

Table 1 (continued)

Z	el.	A	N	$\delta\langle r^2 \rangle$ (fm ²)	$\Delta\delta\langle r^2 \rangle$ (fm ²)	R (fm)	$\Delta_{\text{rot}} R$ (fm)	ΔR_{rel}
		123	73	0.140	0.001	4.6665	0.0023	0.0001
		124	74	0.2008	0.0001	4.6735	0.0023	0.0001
		125	75	0.235	0.003	4.6765	0.0026	0.0003
		126	76	0.290	0.003	4.6833	0.0043	0.0003
		127	77	0.322	0.003	4.6867	0.0048	0.0003
		128	78	0.372	0.004	4.6921	0.0054	0.0004
		129	79	0.384	0.003	4.6934	0.0058	0.0003
		130	80	0.464	0.003	4.7019	0.0066	0.0003
		131	81	0.520	0.004	4.7078	0.0073	0.0004
		132	82	0.534	0.002	4.7093	0.0076	0.0002
51	Sb	121	70			4.6802	0.0026	
		123	72			4.6879	0.0025	
52	Te	116	64	−0.563	0.027	4.6847	0.0128	0.0094
		118	66	−0.457	0.027	4.6956	0.0105	0.0075
		120	68	−0.377	0.006	4.7038	0.0088	0.0070
		122	70	−0.305	0.010	4.7095	0.0031	0.0053
		123	71	−0.289	0.011	4.7117	0.0035	0.0048
		124	72	−0.227	0.009	4.7183	0.0029	0.0039
		125	73	−0.208	0.011	4.7204	0.0030	0.0033
		126	74	−0.153	0.009	4.7266	0.0032	0.0025
		128	76	−0.077	0.004	4.7346	0.0029	0.0012
		130	78	0	0	4.7423	0.0025	0
		132	80	0.076	0.016	4.7500	0.0031	0.0017
		134	82	0.144	0.016	4.7569	0.0041	0.0032
		136	84	0.389	0.019	4.7815	0.0089	0.0071
53	I	127	74			4.7500	0.0081	
54	Xe	116	62	−0.599	0.009	4.7211	0.0096	0.0009
		118	64	−0.460	0.007	4.7387	0.0070	0.0007
		120	66	−0.363	0.007	4.7509	0.0063	0.0007
		122	68	−0.299	0.006	4.7590	0.0059	0.0006
		124	70	−0.242	0.005	4.7661	0.0055	0.0005
		126	72	−0.193	0.007	4.7722	0.0052	0.0007
		127	73	−0.181	0.020	4.7747	0.0038	0.0021
		128	74	−0.152	0.004	4.7774	0.0050	0.0004
		129	75	−0.151	0.001	4.7775	0.0050	0.0003
		130	76	−0.117	0.003	4.7818	0.0049	0.0003
		131	77	−0.125	0.001	4.7808	0.0049	0.0002
		132	78	−0.0844	0.0017	4.7859	0.0048	0.0002
		133	79	−0.106	0.005	4.7831	0.0048	0.0005
		134	80	−0.0518	0.0013	4.7899	0.0047	0.0001
		136	82	0	0	4.7964	0.0047	0
		137	83	0.105	0.003	4.8094	0.0049	0.0003
		138	84	0.254	0.003	4.8279	0.0079	0.0003
		139	85	0.359	0.006	4.8409	0.0100	0.0006
		140	86	0.486	0.002	4.8566	0.0125	0.0002
		141	87	0.591	0.004	4.8694	0.0147	0.0004
		142	88	0.710	0.009	4.8841	0.0169	0.0009
		143	89	0.794	0.004	4.8942	0.0187	0.0004
		144	90	0.908	0.005	4.9082	0.0208	0.0005
		146	92	1.100	0.005	4.9315	0.0245	0.0005
55	Cs	118	63	−0.2044	0.0021	4.7832	0.0092	0.0002
		119	64	−0.1411	0.0062	4.7896	0.0089	0.0006
		120	65	−0.1229	0.0015	4.7915	0.0075	0.0002
		121	66	−0.2650	0.0009	4.7769	0.0078	0.0001
		122	67	−0.2618	0.0016	4.7773	0.0070	0.0002
		123	68	−0.2156	0.0006	4.7820	0.0070	0.0001
		124	69	−0.2083	0.0012	4.7828	0.0062	0.0001
		125	70	−0.1574	0.0006	4.7880	0.0062	0.0001
		126	71	−0.1645	0.0009	4.7872	0.0056	0.0001
		127	72	−0.1022	0.0007	4.7936	0.0055	0.0001
		128	73	−0.1173	0.0004	4.7921	0.0052	0.0001
		129	74	−0.0582	0.0011	4.7981	0.0050	0.0001
		130	75	−0.0482	0.0010	4.7992	0.0049	0.0001
		131	76	−0.0146	0.0007	4.8026	0.0047	0.0001
		132	77	−0.0383	0.0006	4.8002	0.0046	0.0001
		133	78	0	0	4.8041	0.0046	0
		134	79	−0.0100	0.0011	4.8031	0.0046	0.0001
		135	80	0.0259	0.0009	4.8067	0.0047	0.0001
		136	81	0.0174	0.0015	4.8059	0.0052	0.0002
		137	82	0.0852	0.0011	4.8128	0.0050	0.0001
		138	83	0.2099	0.0008	4.8255	0.0050	0.0001
		139	84	0.3739	0.0012	4.8422	0.0069	0.0001
		140	85	0.5051	0.0013	4.8554	0.0088	0.0001

(continued on next page)

Table 1 (continued)

Z	el.	A	N	$\delta(r^2)$ (fm ²)	$\Delta\delta(r^2)$ (fm ²)	R (fm)	$\Delta_{tot}R$ (fm)	ΔR_{rel}
56	Ba	141	86	0.6389	0.0015	4.8689	0.0108	0.0002
		142	87	0.7732	0.0007	4.8825	0.0132	0.0001
		143	88	0.9127	0.0005	4.8965	0.0151	0.0002
		144	89	1.0030	0.0007	4.9055	0.0161	0.0002
		145	90	1.1362	0.0010	4.9188	0.0191	0.0003
		146	91	1.2293	0.0021	4.9281	0.0193	0.0003
		120	64	−0.267	0.010	4.8092	0.0058	0.0010
		121	65	−0.189	0.012	4.8176	0.0052	0.0012
		122	66	−0.212	0.002	4.8153	0.0054	0.0002
		123	67	−0.228	0.002	4.8135	0.0055	0.0002
		124	68	−0.1819	0.0003	4.8185	0.0052	0.0001
		125	69	−0.189	0.002	4.8177	0.0052	0.0002
		126	70	−0.1479	0.0002	4.8221	0.0050	0.0001
		127	71	−0.1641	0.0010	4.8204	0.0051	0.0001
		128	72	−0.1160	0.0003	4.8255	0.0048	0.0001
		129	73	−0.1219	0.0004	4.8248	0.0049	0.0001
		130	74	−0.0895	0.0002	4.8283	0.0047	0.0001
		131	75	−0.0960	0.0003	4.8276	0.0048	0.0001
		132	76	−0.0700	0.0001	4.8303	0.0047	0.0001
		133	77	−0.0873	0.0002	4.8286	0.0047	0.0001
		134	78	−0.0547	0.0001	4.8322	0.0047	0.0001
		135	79	−0.0812	0.0003	4.8294	0.0047	0.0001
		136	80	−0.0422	0.0002	4.8334	0.0046	0.0001
		137	81	−0.0609	0.0002	4.8314	0.0047	0.0001
		138	82	0	0	4.8378	0.0046	0
		139	83	0.129	0.001	4.8513	0.0049	0.0001
		140	84	0.292	0.001	4.8684	0.0059	0.0001
		141	85	0.410	0.001	4.8807	0.0069	0.0001
		142	86	0.550	0.001	4.8953	0.0083	0.0001
		143	87	0.679	0.002	4.9087	0.0096	0.0002
		144	88	0.823	0.003	4.9236	0.0112	0.0003
		145	89	0.928	0.002	4.9345	0.0123	0.0002
		146	90	1.058	0.003	4.9479	0.0138	0.0003
		148	92	1.304	0.006	4.9731	0.0167	0.0006
57	La	135	78	−0.061	0.006	4.8488	0.0060	0.0006
		137	80	−0.048	0.001	4.8496	0.0053	0.0001
		138	81	−0.067	0.001	4.8473	0.0051	0.0001
		139	82	0	0	4.8550	0.0049	0
58	Ce	136	78	−0.031	0.002	4.8739	0.0018	0.0002
		138	80	−0.033	0.002	4.8737	0.0018	0.0002
		140	82	0	0	4.8771	0.0018	0
		142	84	0.281	0.002	4.9063	0.0020	0.0002
		144	86	0.513	0.002	4.9303	0.0024	0.0002
		146	88	0.793	0.002	4.9590	0.0028	0.0002
59	Pr	148	90	1.089	0.002	4.9893	0.0035	0.0002
		141	82			4.8919	0.0050	
60	Nd	132	72	0.050	0.030	4.9174	0.0026	0.0031
		134	74	0.005	0.021	4.9128	0.0026	0.0021
		135	75	−0.037	0.033	4.9086	0.0026	0.0034
		136	76	−0.012	0.027	4.9111	0.0026	0.0027
		137	77	−0.043	0.016	4.9080	0.0026	0.0016
		138	78	−0.006	0.021	4.9123	0.0026	0.0021
		139	79	−0.047	0.014	4.9076	0.0025	0.0014
		140	80	−0.022	0.027	4.9101	0.0026	0.0027
		141	81	−0.066	0.014	4.9057	0.0026	0.0014
		142	82	0	0	4.9123	0.0025	0
		143	83	0.130	0.005	4.9254	0.0026	0.0005
		144	84	0.296	0.003	4.9421	0.0027	0.0003
		145	85	0.410	0.005	4.9535	0.0028	0.0005
		146	86	0.571	0.004	4.9696	0.0030	0.0004
		148	88	0.876	0.004	4.9999	0.0036	0.0004
		150	90	1.282	0.005	5.0400	0.0044	0.0005
62	Sm	138	76	0.067	0.015	4.9599	0.0034	0.0015
		139	77	0.027	0.014	4.9556	0.0034	0.0014
		140	78	0.037	0.015	4.9565	0.0034	0.0015
		141	79	0.030	0.023	4.9517	0.0034	0.0023
		142	80	−0.007	0.013	4.9518	0.0034	0.0013
		143	81	−0.043	0.015	4.9479	0.0034	0.0015
		144	82	0	0	4.9524	0.0034	0
		145	83	0.1167	0.0016	4.9651	0.0034	0.0005
		146	84	0.2732	0.0008	4.9808	0.0035	0.0010
		147	85	0.3669	0.0004	4.9892	0.0035	0.0016
		148	86	0.5199	0.0004	5.0042	0.0034	0.0021

(continued on next page)

Table 1 (continued)

Z	el.	A	N	$\delta\langle r^2 \rangle$ (fm ²)	$\Delta\delta\langle r^2 \rangle$ (fm ²)	R (fm)	$\Delta_{\text{rot}} R$ (fm)	ΔR_{rel}
63	Eu	149	87	0.6125	0.0004	5.0134	0.0035	0.0024
		150	88	0.8240	0.0004	5.0387	<u>0.0048</u>	0.0031
		151	89	0.9800	0.0008	5.0550	<u>0.0057</u>	0.0038
		152	90	1.2493	0.0003	5.0819	<u>0.0060</u>	0.0038
		153	91	1.3490	0.0005	5.0925	<u>0.0068</u>	0.0002
		154	92	1.4806	0.0004	5.1053	<u>0.0067</u>	0.0040
		137	74	0.099	0.043	4.9762	0.0095	0.0046
		138	75	0.115	0.042	4.9779	0.0094	0.0045
		139	76	0.081	0.046	4.9760	0.0093	0.0048
		140	77	0.0295	0.0021	4.9695	0.0091	0.0017
		141	78	0.0323	0.0011	4.9697	0.0091	0.0013
		142	79	−0.056	0.003	4.9607	0.0091	0.0010
		143	80	−0.027	0.001	4.9636	0.0091	0.0007
		144	81	−0.051	0.002	4.9612	0.0091	0.0004
		145	82	0	0	4.9663	0.0091	0
		146	83	0.1248	0.0019	4.9789	0.0092	0.0004
		147	84	0.2718	0.001	4.9938	0.0094	0.0006
		148	85	0.3787	0.0017	5.0045	0.0097	0.0010
		149	86	0.5338	0.001	5.0202	0.0103	0.0013
		150	87	0.6278	0.0013	5.0296	0.0108	0.0016
		151	88	0.8538	0.0011	5.0522	0.0046	0.0018
		152	89	1.3989	0.0034	5.1064	0.0066	0.0021
		153	90	1.4554	0.0017	5.1115	0.0062	0.0024
		154	91	1.588	0.006	5.1239	0.0079	0.0006
		155	92	1.567	0.008	5.1221	0.0069	0.0008
		156	93	1.612	0.008	5.1264	0.0071	0.0009
		157	94	1.702	0.007	5.1351	0.0075	0.0010
		158	95	1.765	0.008	5.1413	0.0078	0.0011
		159	96	1.852	0.008	5.1498	0.0084	0.0012
64	Gd	145	81	−1.915	0.029	4.9786	0.0077	0.0029
		146	82	−1.914	0.015	4.9801	0.0140	0.0015
		148	84	−1.617	0.015	5.0080	0.0171	0.0015
		150	86	−1.358	0.015	5.0342	0.0159	0.0015
		152	88	−1.01	0.001	5.0774	0.0048	0.0001
		154	90	−0.5338	0.0003	5.1223	0.0040	0.0001
		155	91	−0.4309	0.0002	5.1319	0.0041	0.0001
		156	92	−0.3229	0.0002	5.1420	0.0042	0.0001
		157	93	−0.2918	0.0001	5.1449	0.0042	0.0001
		158	94	−0.1643	0.0001	5.1569	0.0043	0.0001
		160	96	0	0	5.1734	0.0044	0
65	Tb	147	82	−1.393	0.012	4.9201	0.1508	0.0032
		148	83	−1.304	0.011	4.9291	0.1507	0.0030
		149	84	−1.175	0.009	4.9427	0.1506	0.0027
		150	85	−1.100	0.009	4.9499	0.1505	0.0025
		151	86	−0.969	0.008	4.9630	0.1504	0.0022
		152	87	−0.909	0.008	4.9689	0.1504	0.0021
		153	88	−0.655	0.008	4.9950	0.1502	0.0016
		154	89	−0.272	0.018	5.0333	0.1501	0.0019
		155	90	−0.215	0.009	5.0391	0.1500	0.0010
		157	92	−0.116	0.008	5.0489	0.1500	0.0009
		159	94	0	0	5.0600	0.1500	0
66	Dy	146	80	−0.018	0.002	5.0438	0.2389	0.0002
		148	82	0	0	5.0455	0.2389	0
		149	83	0.119	0.013	5.0567	0.2394	0.0012
		150	84	0.268	0.026	5.0706	0.2413	0.0026
		151	85	0.370	0.037	5.0801	0.2435	0.0036
		152	86	0.530	0.053	5.0950	0.2482	0.0051
		153	87	0.621	0.062	5.1035	0.2516	0.0060
		154	88	0.844	0.084	5.1241	0.2618	0.0082
		155	89	1.077	0.108	5.1457	0.2751	0.0103
		156	90	1.257	0.126	5.1622	0.2869	0.0123
		157	91	1.352	0.135	5.1709	0.2936	0.0133
		158	92	1.468	0.147	5.1815	0.3023	0.0144
		159	93	1.478	0.148	5.1825	0.3031	0.0144
		160	94	1.616	0.162	5.1951	0.3139	0.0155
		161	95	1.647	0.165	5.1962	0.0459	0.0159
		162	96	1.753	0.175	5.2074	0.0172	0.0169
		163	97	1.806	0.181	5.2099	0.0120	0.0169
		164	98	1.901	0.190	5.2218	0.0106	0.0179
67	Ho	151	84	−1.709	0.008	5.0398	0.0354	0.0008
		152	85	−1.486	0.006	5.0614	0.0343	0.0006
		153	86	−1.324	0.005	5.0760	0.0339	0.0005
		154	87	−1.234	0.003	5.0856	0.0333	0.0003

(continued on next page)

Table 1 (continued)

Z	el.	A	N	$\delta(r^2)$ (fm ²)	$\Delta\delta(r^2)$ (fm ²)	R (fm)	$\Delta_{tot}R$ (fm)	ΔR_{rel}
		155	88	−1.003	0.003	5.1076	0.0326	0.0003
		156	89	−0.881	0.003	5.1156	0.0326	0.0003
		157	90	−0.518	0.002	5.1535	0.0316	0.0002
		158	91	−0.48	0.004	5.1571	0.0316	0.0004
		159	92	−0.37	0.002	5.1675	0.0314	0.0002
		160	93	−0.384	0.003	5.1662	0.0315	0.0003
		161	94	−0.253	0.002	5.1785	0.0313	0.0002
		162	95	−0.219	0.008	5.1817	0.0313	0.0008
		163	96	−0.123	0.006	5.1907	0.0313	0.0006
		165	98	0	0	5.2022	0.0312	0
		150	82	−2.114	0.013	5.0548	0.0254	0.0030
		152	84	−1.846	0.013	5.0843	0.0257	0.0027
		154	86	−1.584	0.002	5.1129	0.0268	0.0021
		156	88	−1.307	0.001	5.1429	0.0285	0.0018
68	Er	158	90	−1.001	0.001	5.1761	0.0312	0.0015
		160	92	−0.738	0.001	5.2045	0.0336	0.0012
		162	94	−0.551	0.001	5.2246	0.0040	0.0010
		164	96	−0.392	0.001	5.2389	0.0035	0.0007
		166	98	−0.263	0.001	5.2516	0.0031	0.0005
		167	99	−0.218	0.001	5.2560	0.0031	0.0004
		168	100	−0.132	0.001	5.2644	0.0035	0.0002
		170	102	0	0	5.2789	0.0041	0
		153	84	−1.708	0.033	5.0643	0.0190	0.0030
		154	85	−1.609	0.015	5.0755	0.0166	0.0019
		156	87	−1.359	0.009	5.0976	0.0135	0.0006
		157	88	−1.157	0.005	5.1140	0.0074	0.0008
		158	89	−1.058	0.006	5.1235	0.0069	0.0007
		159	90	−0.898	0.003	5.1392	0.0060	0.0004
69	Tm	160	91	−0.783	0.003	5.1504	0.0055	0.0004
		161	92	−0.667	0.002	5.1616	0.0050	0.0003
		162	93	−0.567	0.003	5.1713	0.0048	0.0005
		163	94	−0.427	0.002	5.1849	0.0042	0.0002
		164	95	−0.368	0.003	5.1906	0.0042	0.0006
		165	96	−0.265	0.002	5.2004	0.0038	0.0002
		166	97	−0.221	0.003	5.2046	0.0038	0.0003
		167	98	−0.134	0.002	5.2129	0.0036	0.0003
		168	99	−0.092	0.004	5.2170	0.0036	0.0004
		169	100	0	0	5.2256	0.0035	0
		170	101	0.048	0.001	5.2303	0.0036	0.0005
		171	102	0.139	0.005	5.2388	0.0037	0.0006
		172	103	0.164	0.022	5.2411	0.0052	0.0030
70	Yb	152	82	−2.746	0.004	5.0423	0.0146	0.0028
		154	84	−2.335	0.005	5.0875	0.0105	0.0026
		155	85	−2.181	0.007	5.1040	0.0110	0.0010
		156	86	−2.015	0.002	5.1219	0.0103	0.0023
		157	87	−1.908	0.009	5.1324	0.0100	0.0035
		158	88	−1.737	0.001	5.1498	0.0088	0.0006
		159	89	−1.618	0.009	5.1629	0.0084	0.0022
		160	90	−1.462	0.001	5.1781	0.0076	0.0004
		161	91	−1.353	0.001	5.1889	0.0072	0.0003
		162	92	−1.191	0.001	5.2054	0.0067	0.0003
		163	93	−1.089	0.001	5.2157	0.0064	0.0002
		164	94	−0.942	0.001	5.2307	0.0060	0.0003
		165	95	−0.8473	0.0003	5.2399	0.0058	0.0002
		166	96	−0.7220	0.0004	5.2525	0.0057	0.0001
71	Lu	167	97	−0.6252	0.0003	5.2621	0.0056	0.0001
		168	98	−0.5406	0.0003	5.2702	0.0056	0.0001
		169	99	−0.4692	0.0003	5.2771	0.0056	0.0007
		170	100	−0.3845	0.0001	5.2853	0.0056	0.0001
		171	101	−0.3273	0.0001	5.2906	0.0057	0.0001
		172	102	−0.2366	0.0001	5.2995	0.0058	0.0002
		173	103	−0.1810	0.0001	5.3046	0.0059	0.0002
		174	104	−0.1159	0.0001	5.3108	0.0060	0.0003
		175	105	−0.0827	0.0074	5.3135	0.0061	0.0002
		176	106	0	0	5.3215	0.0062	0
		161	90	−1.5083	0.0013	5.2293	0.0320	0.0003
		162	91	−1.3966	0.0012	5.2398	0.0317	0.0003
		163	92	−1.2174	0.0012	5.2567	0.0312	0.0003
		164	93	−1.1006	0.0012	5.2677	0.0310	0.0002
		165	94	−0.9372	0.0007	5.2830	0.0307	0.0002
		166	95	−0.7851	0.0008	5.2972	0.0305	0.0001
		167	96	−0.6397	0.0007	5.3108	0.0303	0.0001
		168	97	−0.5124	0.0010	5.3227	0.0302	0.0001

(continued on next page)

Table 1 (continued)

Z	el.	A	N	$\delta\langle r^2 \rangle$ (fm ²)	$\Delta\delta\langle r^2 \rangle$ (fm ²)	R (fm)	$\Delta_{\text{rot}} R$ (fm)	ΔR_{rel}
72	Hf	169	98	−0.4443	0.0006	5.3290	0.0302	0.0001
		170	99	−0.3644	0.0006	5.3364	0.0302	0.0001
		171	100	−0.2863	0.0007	5.3436	0.0302	0.0001
		172	101	−0.2323	0.0007	5.3486	0.0302	0.0001
		173	102	−0.1340	0.0010	5.3577	0.0303	0.0001
		174	103	−0.0718	0.0006	5.3634	0.0303	0.0001
		175	104	0	0	5.3700	0.0304	0
		176	105	0.0425	0.0010	5.3739	0.0304	0.0002
		177	106	0.1248	0.0009	5.3815	0.0305	0.0002
		178	107	0.1714	0.0010	5.3857	0.0306	0.0002
		179	108	0.2357	0.0010	5.3917	0.0307	0.0002
		170	98	−0.494	0.009	5.2898	0.0055	0.0009
		171	99	−0.366	0.005	5.3041	0.0049	0.0008
		172	100	−0.322	0.006	5.3065	0.0043	0.0007
		173	101	−0.244	0.004	5.3140	0.0038	0.0005
		174	102	−0.180	0.003	5.3201	0.0035	0.0004
		175	103	−0.091	0.002	5.3191	0.0036	0.0010
		176	104	−0.091	0.001	5.3286	0.0032	0.0002
		177	105	−0.065	0.001	5.3309	0.0031	0.0001
		178	106	0	0	5.3371	0.0031	0
		179	107	0.039	0.002	5.3408	0.0031	0.0001
73	Ta	180	108	0.040	0.005	5.3470	0.0032	0.0002
		182	110	0.176	0.005	5.3516	0.0036	0.0005
		181	108			5.3507	0.0034	
		180	106	−0.169	0.006	5.3491	0.0022	0.0017
		182	108	−0.099	0.005	5.3559	0.0017	0.0010
74	W	183	109	−0.047	0.006	5.3611	0.0020	0.0007
		184	110	0	0	5.3658	0.0023	0
		186	112	0.086	0.004	5.3743	0.0026	0.0009
		185	110	0	0	5.3596	0.0172	0
75	Re	187	112	0.110	0.010	5.3698	0.0173	0.0009
		184	108	−0.320	0.018	5.3823	0.0022	0.0017
76	Os	186	110	−0.231	0.015	5.3909	0.0017	0.0014
		187	111	−0.205	0.016	5.3933	0.0018	0.0015
		188	112	−0.144	0.011	5.3993	0.0011	0.0010
		189	113	−0.119	0.012	5.4016	0.0012	0.0011
		190	114	−0.068	0.006	5.4062	0.0013	0.0006
		192	116	0	0	5.4126	0.0015	0
		182	105	−0.283	0.006	5.3705	0.1061	0.0007
77	Ir	183	106	−0.203	0.004	5.3780	0.1061	0.0005
		184	107	−0.176	0.003	5.3805	0.1061	0.0004
		185	108	−0.123	0.003	5.3854	0.1061	0.0003
		186	109	−0.073	0.004	5.3900	0.1061	0.0004
		187	110	−0.168	0.003	5.3812	0.1061	0.0004
		188	111	−0.140	0.004	5.3838	0.1061	0.0004
		189	112	−0.076	0.002	5.3898	0.1061	0.0002
		191	114	0	0	5.3968	0.1061	0
		193	116	0.069	0.001	5.4032	0.1061	0.0001
		178	100	−0.529	0.016	5.3728	0.0066	0.0015
		179	101	−0.335	0.021	5.3915	0.0050	0.0019
		180	102	−0.360	0.011	5.3891	0.0049	0.0010
78	Pt	181	103	−0.251	0.015	5.3996	0.0041	0.0014
		182	104	−0.279	0.010	5.3969	0.0041	0.0009
		183	105	−0.196	0.020	5.4038	0.0036	0.0019
		184	106	−0.240	0.018	5.4015	0.0036	0.0017
		185	107	−0.090	0.005	5.4148	0.0028	0.0005
		186	108	−0.213	0.004	5.4037	0.0036	0.0004
		187	109	−0.188	0.004	5.4063	0.0037	0.0004
		188	110	−0.193	0.003	5.4053	0.0034	0.0003
		189	111	−0.187	0.005	5.4060	0.0035	0.0005
		190	112	−0.137	0.002	5.4108	0.0030	0.0002
		191	113	−0.142	0.004	5.4102	0.0031	0.0004
		192	114	−0.073	0.002	5.4169	0.0028	0.0002
		193	115	−0.047	0.006	5.4191	0.0027	0.0006
		194	116	0	0	5.4236	0.0025	0
		195	117	0.036	0.002	5.4270	0.0026	0.0002
		196	118	0.075	0.002	5.4307	0.0027	0.0002
		198	120	0.154	0.002	5.4383	0.0032	0.0002
		183	104	−0.140	0.009	5.4247	0.0043	0.0008
		184	105	−0.077	0.007	5.4306	0.0041	0.0011
		185	106	−0.088	0.004	5.4296	0.0041	0.0008
		186	107	−0.024	0.008	5.4354	0.0039	0.0007

(continued on next page)

Table 1 (continued)

Z	el.	A	N	$\delta(r^2)$ (fm ²)	$\Delta\delta(r^2)$ (fm ²)	R (fm)	$\Delta_{tot}R$ (fm)	ΔR_{rel}
80	Hg	187	108	−0.382	0.005	5.4018	0.0058	0.0008
		188	109	−0.352	0.006	5.4049	0.0055	0.0008
		189	110	−0.313	0.004	5.4084	0.0052	0.0006
		190	111	−0.284	0.005	5.4109	0.0049	0.0006
		191	112	−0.245	0.001	5.4147	0.0046	0.0004
		192	113	−0.211	0.002	5.4179	0.0044	0.0003
		193	114	−0.164	0.001	5.4221	0.0042	0.0002
		194	115	−0.131	0.001	5.4252	0.0040	0.0002
		195	116	−0.079	0.004	5.4298	0.0040	0.0006
		196	117	−0.043	0.005	5.4332	0.0039	0.0004
		197	118	0	0	5.4371	0.0038	0
		198	119	0.031	0.002	5.4400	0.0038	0.0002
		199	120	0.090	0.001	5.4454	0.0039	0.0001
		181	101	−0.114	0.004	5.4364	0.0032	0.0004
		182	102	−0.693	0.021	5.3833	0.0052	0.0020
		183	103	−0.070	0.004	5.4405	0.0031	0.0004
		184	104	−0.550	0.002	5.3949	0.0047	0.0002
		185	105	−0.077	0.001	5.4397	0.0031	0.0001
		186	106	−0.477	0.001	5.4017	0.0043	0.0001
		187	107	−0.447	0.002	5.4046	0.0042	0.0002
		188	108	−0.404	0.001	5.4085	0.0040	0.0001
		189	109	−0.387	0.002	5.4100	0.0040	0.0002
		190	110	−0.326	0.001	5.4158	0.0037	0.0001
		191	111	−0.313	0.004	5.4171	0.0037	0.0004
		192	112	−0.246	0.001	5.4232	0.0035	0.0001
		193	113	−0.242	0.009	5.4238	0.0035	0.0008
		194	114	−0.164	0.001	5.4309	0.0033	0.0001
		195	115	−0.126	0.005	5.4345	0.0032	0.0005
		196	116	−0.0825	0.0001	5.4385	0.0031	0.0001
		197	117	−0.054	0.003	5.4412	0.0031	0.0003
		198	118	0	0	5.4463	0.0031	0
		199	119	0.0130	0.0001	5.4474	0.0031	0.0002
		200	120	0.0942	0.0001	5.4551	0.0031	0.0003
		201	121	0.1258	0.0001	5.4581	0.0032	0.0003
		202	122	0.1981	0.0001	5.4648	0.0033	0.0003
		203	123	0.231	0.004	5.4679	0.0035	0.0003
		204	124	0.3001	0.0001	5.4744	0.0036	0.0003
		205	125	0.333	0.002	5.4776	0.0038	0.0003
		206	126	0.397	0.002	5.4837	0.0040	0.0003
81	Tl	188	107	−0.7708	0.0005	5.4017	0.0072	0.0013
		190	109	−0.6693	0.0003	5.4121	0.0056	0.0013
		191	110	−0.6201	0.0007	5.4169	0.0048	0.0003
		192	111	−0.5967	0.0003	5.4191	0.0051	0.0012
		193	112	−0.542	0.011	5.4243	0.0042	0.0008
		194	113	−0.5261	0.0005	5.4259	0.0046	0.0010
		195	114	−0.457	0.007	5.4325	0.0039	0.0006
		196	115	−0.4546	0.0005	5.4327	0.0042	0.0009
		197	116	−0.391	0.001	5.4388	0.0036	0.0002
		198	117	−0.383	0.007	5.4396	0.0036	0.0006
		199	118	−0.296	0.007	5.4479	0.0031	0.0006
		200	119	−0.283	0.007	5.4491	0.0031	0.0006
		201	120	−0.197	0.001	5.4573	0.0029	0.0004
		202	121	−0.174	0.007	5.4595	0.0027	0.0006
		203	122	−0.0978	0.0001	5.4666	0.0027	0.0002
		204	123	−0.060	0.007	5.4704	0.0028	0.0006
		205	124	0	0	5.4759	0.0026	0
		207	126	0.0993	0.0002	5.4853	0.0027	0.0002
		208	127	0.185	0.013	5.4946	0.0028	0.0012
82	Pb	182	100	−1.311	0.013	5.3788	0.0035	0.0012
		183	101	−1.225	0.008	5.3869	0.0030	0.0007
		184	102	−1.160	0.005	5.3930	0.0029	0.0005
		185	103	−1.103	0.008	5.3984	0.0028	0.0007
		186	104	−1.057	0.005	5.4027	0.0027	0.0005
		187	105	−1.002	0.006	5.4079	0.0026	0.0006
		188	106	−0.938	0.006	5.4139	0.0025	0.0006
		189	107	−0.898	0.008	5.4177	0.0024	0.0007
		190	108	−0.851	0.002	5.4222	0.0023	0.0005
		191	109	−0.845	0.004	5.4229	0.0026	0.0011
		192	110	−0.766	0.005	5.4300	0.0025	0.0011
		193	111	−0.756	0.003	5.4310	0.0023	0.0007
		194	112	−0.689	0.004	5.4372	0.0023	0.0009
		195	113	−0.671	0.004	5.4389	0.0045	0.0011
		196	114	−0.611	0.005	5.4444	0.0024	0.0014
		197	115	−0.609	0.003	5.4446	0.0024	0.0014

(continued on next page)

Table 1 (continued)

Z	el.	A	N	$\delta\langle r^2 \rangle$ (fm ²)	$\Delta\delta\langle r^2 \rangle$ (fm ²)	R (fm)	$\Delta_{\text{rot}} R$ (fm)	ΔR_{rel}
83	Bi	198	116	−0.5258	0.0002	5.4524	0.0022	0.0012
		199	117	−0.5206	0.0005	5.4529	0.0022	0.0012
		200	118	−0.4322	0.0002	5.4611	0.0020	0.0010
		201	119	−0.4127	0.0003	5.4629	0.0019	0.0009
		202	120	−0.3307	0.0002	5.4705	0.0017	0.0007
		203	121	−0.3071	0.0003	5.4727	0.0017	0.0007
		204	122	−0.2249	0.0001	5.4803	0.0014	0.0005
		205	123	−0.1983	0.0002	5.4828	0.0015	0.0005
		206	124	−0.1189	0.0001	5.4902	0.0014	0.0003
		207	125	−0.0743	0.0001	5.4943	0.0014	0.0002
		208	126	0	0	5.5012	0.0013	0
		209	127	0.0945	0.0005	5.5100	0.0014	0.0003
		210	128	0.2125	0.0002	5.5208	0.0016	0.0007
		211	129	0.3020	0.0003	5.5290	0.0017	0.0007
		212	130	0.4178	0.0016	5.5396	0.0019	0.0003
		214	132	0.6150	0.0011	5.5577	0.0023	0.0002
		202	119	−0.408	0.002	5.4840	0.0069	0.0002
		203	120	−0.330	0.002	5.4911	0.0058	0.0002
		204	121	−0.305	0.003	5.4934	0.0055	0.0003
		205	122	−0.224	0.001	5.5008	0.0044	0.0001
		206	123	−0.196	0.001	5.5034	0.0040	0.0001
		207	124	−0.119	0.002	5.5103	0.0032	0.0002
		208	125	−0.071	0.002	5.5147	0.0028	0.0002
		209	126	0	0	5.5211	0.0026	0
		210	127	0.099	0.003	5.5300	0.0030	0.0003
		212	129	0.307	0.004	5.5489	0.0054	0.0004
		213	130	0.416	0.001	5.5586	0.0069	0.0001
84	Po	192	108	−0.403	0.019	5.5220	0.0178	0.0017
		194	110	−0.462	0.016	5.5167	0.0178	0.0014
		196	112	−0.496	0.013	5.5136	0.0178	0.0012
		198	114	−0.485	0.017	5.5146	0.0178	0.0015
		200	116	−0.426	0.014	5.5199	0.0178	0.0013
		202	118	−0.336	0.015	5.5281	0.0177	0.0014
		204	120	−0.229	0.014	5.5378	0.0177	0.0013
		205	121	−0.216	0.014	5.5389	0.0177	0.0013
		206	122	−0.116	0.014	5.5480	0.0177	0.0013
		207	123	−0.092	0.014	5.5501	0.0177	0.0013
		208	124	0	0	5.5584	0.0176	0
		209	125	0.049	0.012	5.5628	0.0176	0.0011
		210	126	0.134	0.010	5.5704	0.0176	0.0009
		216	132	0.867	0.014	5.6359	0.0174	0.0012
		218	134	1.092	0.015	5.6558	0.0173	0.0013
		202	116	−0.4382	0.0004	5.5521	0.0181	0.0001
		204	118	−0.3860	0.0003	5.5568	0.0180	0.0001
		205	119	−0.3849	0.0003	5.5569	0.0180	0.0001
86	Rn	206	120	−0.3058	0.0003	5.5640	0.0178	0.0001
		207	121	−0.2926	0.0002	5.5652	0.0178	0.0001
		208	122	−0.2125	0.0002	5.5725	0.0177	0.00004
		209	123	−0.1917	0.0001	5.5743	0.0177	0.00003
		210	124	−0.1143	0.0001	5.5813	0.0177	0.00002
		211	125	−0.0735	0.0001	5.5850	0.0176	0.00001
		212	126	0	0	5.5915	0.0176	0
		218	132	0.7000	0.0003	5.6540	0.0187	0.0001
		219	133	0.8212	0.0003	5.6648	0.0191	0.0001
		220	134	0.9151	0.0003	5.6731	0.0194	0.0002
		221	135	1.0320	0.0004	5.6834	0.0199	0.0002
		222	136	1.1236	0.0004	5.6915	0.0203	0.0002
		207	120	−0.21794	0.00016	5.5720	0.0176	0.00004
		208	121	−0.20804	0.00012	5.5729	0.0176	0.00003
87	Fr	209	122	−0.13043	0.00008	5.5799	0.0176	0.00002
		210	123	−0.10831	0.00004	5.5818	0.0176	0.00002
		211	124	−0.03757	0.00004	5.5882	0.0176	0.00001
		212	125	0	0	5.5915	0.0176	0
		213	126	0.06829	0.00008	5.5977	0.0176	0.00001
		220	133	0.86725	0.00045	5.6688	0.0177	0.0001
		221	134	0.98269	0.00033	5.6790	0.0177	0.0002
		222	135	1.09543	0.00012	5.6890	0.0177	0.0002
		223	136	1.16507	0.00008	5.6951	0.0178	0.0002
		224	137	1.28937	0.00004	5.7061	0.0178	0.0002
		225	138	1.34862	0.00022	5.7112	0.0178	0.0002
		226	139	1.43700	0.00004	5.7190	0.0178	0.0002
		227	140	1.60249	0.00008	5.7335	0.0179	0.0002

(continued on next page)

Table 1 (continued)

Z	el.	A	N	$\delta(r^2)$ (fm ²)	$\Delta\delta(r^2)$ (fm ²)	R (fm)	$\Delta_{tot}R$ (fm)	ΔR_{rel}
88	Ra	228	141	1.67522	0.00020	5.7399	0.0179	0.0003
		208	120	−0.2560	0.0002	5.5850	0.0183	0.0024
		209	121	−0.2530	0.0002	5.5853	0.0182	0.0022
		210	122	−0.1820	0.0002	5.5917	0.0180	0.0017
		211	123	−0.1680	0.0001	5.5929	0.0179	0.0015
		212	124	−0.0990	0.0001	5.5991	0.0177	0.0009
		213	125	−0.0660	0.0001	5.6020	0.0177	0.0006
		214	126	0	0	5.6079	0.0177	0
		220	132	0.6790	0.0002	5.6683	0.0215	0.0062
		221	133	0.8050	0.0002	5.6795	0.0228	0.0073
		222	134	0.8950	0.0002	5.6874	0.0239	0.0081
		223	135	1.0070	0.0003	5.6973	0.0253	0.0091
		224	136	1.0900	0.0003	5.7046	0.0263	0.0098
		225	137	1.2080	0.0003	5.7150	0.0279	0.0108
		226	138	1.2770	0.0003	5.7211	0.0288	0.0115
		227	139	1.3650	0.0004	5.7283	0.0300	0.0123
		228	140	1.4590	0.0004	5.7370	0.0315	0.0131
		229	141	1.5560	0.0005	5.7455	0.0329	0.0140
		230	142	1.6670	0.0005	5.7551	0.0346	0.0150
		232	144	1.8540	0.0005	5.7714	0.0375	0.0166
90	Th	227	137	−0.508	0.003	5.7404	0.0165	0.0062
		228	138	−0.413	0.001	5.7488	0.0152	0.0049
		229	139	−0.334	0.001	5.7557	0.0143	0.0040
		230	140	−0.2050	0.0004	5.7670	0.0131	0.0025
		232	142	0	0	5.7848	0.0124	0
92	U	233	141	−0.435	0.001	5.8203	0.0049	0.0043
		234	142	−0.334	0.001	5.8291	0.0052	0.0033
		235	143	−0.2803	0.0002	5.8337	0.0041	0.0027
		236	144	−0.1676	0.0002	5.8431	0.0038	0.0016
		238	146	0	0	5.8571	0.0033	0
94	Pu	238	144	−0.082	0.004	5.8535	0.0378	0.0012
		239	145	0	0	5.8601	0.0378	0
		240	146	0.122	0.003	5.8701	0.0379	0.0016
		241	147	0.179	0.004	5.8748	0.0379	0.0019
		242	148	0.273	0.004	5.8823	0.0380	0.0024
95	Am	244	150	0.426	0.008	5.8948	0.0382	0.0032
		241	146	−0.142	0.008	5.8928	0.0042	0.0012
		243	148	0	0	5.9048	0.0035	0
96	Cm	242	146	−0.168	0.056	5.8285	0.0192	0.0049
		244	148	0	0	5.8429	0.0181	0
		245	149	0.054	0.011	5.8475	0.0182	0.0010
		246	150	0.156	0.022	5.8562	0.0184	0.0020
		248	152	0.303	0.054	5.8687	0.0193	0.0040

Table 2

Parameters used for the extraction of radii changes from OIS.

¹ H	IS on 1S → 2S transition; $\delta\langle r^2 \rangle^{1,2}$ as given by [Pa10].
² He	He I at 389 nm, $2^3S_1 \rightarrow 3^3P_2$ transition; $\delta\langle r^2 \rangle$ [Wa04, Mu07]; $F_{cal} = +1.008$ MHz/fm ² , $MS_{cal}({}^{4,6}\text{He}) = +43196.217$ MHz (see for details [Dr04]).
³ Li	Li I at 735 nm ($2s^2S_{1/2} - 3s^2S_{1/2}$ —two photon transition); $\delta\langle r^2 \rangle$ as given by [Nö11, 28] (see also [Ew04, Sá06, Sá06b]); $F_{cal} = -1.5719(16)$ MHz/fm ² , $MS_{cal} = +11452.821(3)$ MHz for $\delta\langle r^2 \rangle^{6,7}$ [Nö11, 28] (the latest version of F and MS calculations); the OIS experimental technique is accompanied by high-precision theoretical calculations.
⁴ Be	Be I at D ₁ and D ₂ -lines; $\delta\langle r^2 \rangle$ [Nö 09, Žá10]; $F_{cal}(D_1) = -16.912$ MHz/fm ² , $MS_{cal}({}^{9,7}\text{Be}) = -49225.765$ MHz [Ya08]; $F_{cal}(D_2) \approx +17$ MHz/fm ² (for details see [Pu08]), $MS_{cal}({}^{9,7}\text{Be}) = -49231.827(39)$ MHz [Ya08].
¹⁰ Ne	IS for Ne I at 614.3 nm, transition $2p^5 3s[3/2]_2 \rightarrow 2p^5 3p[3/2]_2$; $\delta\langle r^2 \rangle$ as given by [Ge08, Ma11]; $F_{se} = -40(4)$ MHz/fm ² , $MS_{\mu} = +363(42)$ GHz u calibrated via King plot with R_{μ} -data of [4].
¹¹ Na	IS for Na I at D ₁ -line; $\delta\langle r^2 \rangle$ [5]; $F_{se} = -47$ MHz/fm ² ; $MS_{se} = +385.5$ GHz u [Hu82].
¹⁸ Ar	IS for Ar I at 763.7 nm, transition $3p^5 4s[3/2]_2 \rightarrow 3p^5 4p[3/2]_2$ [Kl96, Bl08]; $\delta\langle r^2 \rangle$ [Bl08] with $F_{se} = -104(10)$ MHz/fm ² ; $MS_{\mu} = +189.0(1.9)$ —calibrated via King plot using R_{μ} -data of [4].
¹⁹ K	IS for K I at D ₁ -line; $\delta\langle r^2 \rangle$ [To82], $F_{se} = -128$ MHz/fm ² ; $MS_{e\mu} = +198.4(3.9)$ GHz u—King plot procedure using model independent $R_{e\mu}$ data from [Wo81].
²⁰ Ca	IS for ^{40–48} Ca I at different transition; $\delta\langle r^2 \rangle$ from [Pa84], $F_{e\mu}$, $MS_{e\mu}$ —via King plot procedure using $R_{e\mu}$ data from [Wo81]; IS(^{40,39} Ca) [Ve96] and IS(^{44,50} Ca) [Ve92] for CaII at 397 nm, transition $3p^6 4s^2 S_{1/2} \rightarrow 3p^6 4p^2 P_{1/2}$; $F_{cal} = -283(6)$ MHz/fm ² [Mä92], $MS_{e\mu} = +405.1(3.8)$ GHz u from King-plot procedure versus OIS data of [Pa84].
²¹ Sc	Sc II at 363.1 nm, transition $3d 4s^3 D_2 \rightarrow 3d 4p^3 F_3$, $F_{cal} = -355(50)$ MHz/fm ² , $MS_{cal} = +583(30)$ GHz u [Av11].
²² Ti	IS for Ti II at 324.2 nm, transition $d^2 s^4 F_{3/2} \rightarrow d^2 p^4 F_{3/2}$ [Ga04]; $F_{cal} = -460(46)$ MHz/fm ² , $MS_{e\mu} = +788(6)$ GHz u calibrated by model independent $R_{e\mu}$ -data of [Wo81].
²⁴ Cr	$\delta\langle r^2 \rangle$ recalculated with isotopic shifts of Cr I—projected values on 520.8 nm (transition $3d^5 4s^5 S_2 \rightarrow 3d^5 4p^5 P_3$) [14], $F_{e\mu} = +244.6(34.5)$ MHz/fm ² , $MS_{e\mu} = -475.4(9.4)$ GHz u calibrated via King-plot using $R_{e\mu}$ -data of [15].
²⁵ Mn	IS for Mn II at 294.9 nm, transition $3d^5 4s^5 S_2 \rightarrow 3d^5 4p^5 P_3$, $\delta\langle r^2 \rangle$ calculated with $F_{cal} = -572$ MHz/fm ² , $MS_{cal} = +852$ GHz u [Ch10].
²⁶ Fe	IS for Fe I at 304.76 nm, transition $3d^6 4s^2 D_2 \rightarrow 3d^7 4p^5 D_3$ [Be97]; $\delta\langle r^2 \rangle$ recalculated with $F_{e\mu} = -920(114)$ MHz/fm ² , $MS_{e\mu} = +2992(50)$ GHz u—calibration via King plot using $R_{e\mu}$ data of [15].
²⁸ Ni	IS for Ni I at 361.05 nm, transition $3d^9 4s^3 D_2 \rightarrow 3d^9 4p^3 P_2$ [St80]; $\delta\langle r^2 \rangle$ recalculated with $F_{se} = -767(77)$ MHz/fm ² ; $MS_{e\mu} = +1228(15)$ GHz u—calibrated via King plot using $R_{e\mu}$ data of [15].
³⁰ Zn	IS for Zn I at 307.6 nm, transition $3d^{10} 4s^2 S_0 \rightarrow 3d^{10} 4s 4p^3 P^1$ [Ca97]; $\delta\langle r^2 \rangle$ recalculated with $F_{cal} = -1510(151)$ MHz/fm ² [Ca97], $MS_{e\mu} = +1970(29)$ GHz u—calibrated via King plot using $R_{e\mu}$ data of [15].
³⁶ Kr	$\delta\langle r^2 \rangle$ as given in [Ke94]; $F_{se} = -608(61)$ MHz/fm ² , $MS_e = +167(19)$ GHz u determined via King plot using R_e data of [Ma84].
³⁷ Rb	IS for Rb I at D ₂ -line; $F_{se} = -650(65)$ MHz/fm ² , $MS_{se} \approx N = +211$ GHz u [Th81].
³⁸ Sr	IS for Sr II at 407.9 nm, transition $5 s^2 S_{1/2} \rightarrow 5 p^2 P_{3/2}$; IS(^{78,79–98,100} Sr) [Bu90]; IS(^{77–88} Sr) [Li92]; IS(⁹⁹ Sr) [Li91]; $F_{se} = -1582(49)$ MHz/fm ² , $MS_{\mu} = +351(44)$ GHz u [Bu90].
³⁹ Y	Y II at 363 nm ($5s^2 S_0 \rightarrow 4d 5p^1 P_1$); $F_{phen} = -3181$ MHz/fm ² , $MS_{phen} = +1789$ GHz u—King plot vs $\delta\langle r^2 \rangle$ of neighboring isotones [Ch07].
⁴⁰ Zr	IS(^{91–102} Zr II) at nm 327 nm ($d^2 s^4 F_3 \rightarrow d^2 p^4 F_5$ transition) [Ca02]; $\delta\langle r^2 \rangle$ recalculated with $F_{e\mu} = -2190(183)$ MHz/fm ² , $MS_e = +737(202)$ GHz u via King plot versus $R_{e\mu}$ data of [8]; IS(^{87–92} Zr II) at 310 nm ($d^2 s^4 F_{3/2} \rightarrow d^2 p^4 D_{3/2}$ transition) [Fo02], $\delta\langle r^2 \rangle$ recalculated with $F_{e\mu}(310 \text{ nm}) = -1762(119)$ MHz/fm ² , $MS_{e\mu} = +385(139)$ GHz u via King plot versus $R_{e\mu}$ data of [8].
⁴¹ Nb	IS for Nb II at 291 nm ($5s^5 F_1 \rightarrow 5p^5 F_1$ transition); $\delta\langle r^2 \rangle$ from [Ch09]; $F_{phen} = -2.43$ GHz/fm ² , $MS_{phen} = +718$ GHz u—using King plot versus $\delta\langle r^2 \rangle$ of neighbouring isotopic chain of Zr.
⁴² Mo	IS for Mo II at 293 nm ($4d^4 5s^6 D_{1/2} \rightarrow 4d^4 5p^6 F_{1/2}$ transition) [Ch09a]; $\delta\langle r^2 \rangle$ recalculated with $F_{\mu} = -2.82(2)$ GHz/fm ² , $MS_{\mu} = +681(197)$ GHz u from King plot using R_{μ} of [8].
⁴⁴ Ru	IS for Ru I at 437 nm ($4d^6 5s^2 D_4 \rightarrow 4d^7 5p^3 F_4$ transition) [Ki64]; $\delta\langle r^2 \rangle$ recalculated with $F_{e\mu} = -4621(581)$ MHz/fm ² , $MS_{e\mu} = +2275(766)$ GHz u from King plot versus $R_{e\mu}$ data of [15].
⁴⁶ Pd	IS for Pd I at 447.4 nm ($4d^9 5s^1 D_2 \rightarrow 4d^9 5p^3 P_2$ transition) [Kü93]; $\delta\langle r^2 \rangle$ recalculated with $F_{\mu e} = -2775(118)$ MHz/fm ² , $MS_{\mu e} = +668(146)$ GHz u—calibrated via King plot versus $A_{\mu e}$ [14].
⁴⁷ Ag	Ag I at 547.7 nm ($4d^9 5s^2 D_{5/2} \rightarrow 4d^{10} 6p^2 P_{3/2}$); $\delta\langle r^2 \rangle$ as given in [Di89], where $F_{se} = -12070(966)$ MHz/fm ² , $MS_{se} = +4446(2700)$ GHz u.
⁴⁸ Cd	IS for Cd I for at 326.1 nm ($4d^{10} 5s^2 S_0 \rightarrow 4d^{10} 5s 5p^3 P_1$) using projected values from [14] (see references therein); $\delta\langle r^2 \rangle$ recalculated with $F_{se} = +3910(460)$ MHz/fm ² , $MS_{se} = +876(230)$ GHz u (see [5] and references therein).
⁴⁹ In	IS for In II at 451 nm ($5s^2 5p^2 P_{3/2} \rightarrow 5s^2 6s^2 S_{1/2}$); $F_{cal} = +2.070(10)$ GHz/fm ² ; $MS_{phen} = -62(73)$ GHz u calibrated using $\delta\langle r^2 \rangle$ for neighbouring isotones [Eb87].
⁵⁰ Sn	Sn I at 286.3 nm ($5s^2 5p^2 P_0 \rightarrow 5s^2 5p 6s^3 P_1$); IS(^{110–125} Sn) [An86]; IS(^{126–132} Sn) [Bl05]; IS(^{108,109} Sn) at 452 nm [Eb87b] calibrated to 286.3 nm; $F_{se} = +3.30(27)$ MHz/fm ² [Ba83]; $MS_{\mu} = -761(200)$ GHz u [Bl05] calibrated using King plot versus R_{μ} data of [Pi90].
⁵² Te	IS for Te II at 214.3 nm ($5p^3 3P_2 \rightarrow 5p^3 6s^3 S_1$) [Ro09], $F_{\mu} = +3.78(48)$ GHz/fm ² , $MS_{\mu} = -556(283)$ GHz [16] calibrated via King plot with R_{μ} data of [4].
⁵⁴ Xe	IS for Xe I at $\lambda = 823.2$ nm ($5p^5 6s[3/2]_2 \rightarrow 5p^5 6p[3/2]_2$); $\delta\langle r^2 \rangle$ ^{116–146} Xe (exceptions ^{127,133} Te) [Bo89]; IS(^{127,133} Xe) projected values on 823.2 nm (see [14] and references therein); $F_{se} = -2.32(23)$ GHz/fm ² , $MS_{se} \approx N = +193(178)$ GHz u [Bo89].
⁵⁵ Cs	IS for Cs I at 852.1 nm ($6s^2 S_{1/2} \rightarrow 6p^2 P_{3/2}$ transition); IS(^{118–145} Cs) [Th81b]; IS(^{118,146} Cs) [Co87]; $F_{se} = -2313(230)$ MHz/fm ² , $MS_{se} \approx N = +193$ GHz u [Th81b].
⁵⁶ Ba	IS for Ba I—projected values on 553.6 nm ($6s^2 S_0 \rightarrow 6s 6p^1 P_1$ transition) (see [14] and references therein); $\delta\langle r^2 \rangle$ recalculated with $F_{se} = -3929(40)$ MHz/fm ² , $MS_{se} \approx N = +295$ GHz u [Be79].
⁵⁷ La	IS for La II at 538.2 nm ($6s^2 S_0 \rightarrow 5d 6p^3 D_1$); $\delta\langle r^2 \rangle$ —recalculated using $F_{se} = -13.15(1.23)$ GHz/fm ² , $MS_{se} = -4106$ GHz u—combined data from [li03, Fi74].
⁵⁸ Ce	IS for Ce II for 331 nm ($5d^2 J = 7/2 \rightarrow 5d 6p J = 7/2$); $F_{se} = +2031(103)$ MHz/fm ² , $MS_{se} = -666(504)$ GHz u [Ch03].
⁶⁰ Nd	IS for Nd I at 588.8 nm ($6s^2 S_{1/2} \rightarrow 6s 6p^3 K_3$); IS(^{132–143} Nd) [Le92]; IS(^{142–150} Nd) [Al87]; $F_{se} = +825$ MHz/fm ² , $MS_{se} = +4547(45)$ GHz u [Le92].
⁶² Sm	$\delta\langle r^2 \rangle$ recalculated using projected values of IS(^{138–154} Sm) for Sm I on 570.7 nm ($4f^6 6s^2 F_1 \rightarrow 4f^6 6s 6p^3 F_0$) (see [14] and references therein), $F_{se} = -4199(389)$ MHz/fm ² , $MS_{se} = -295(13)$ GHz u calculated combining OIS data of [En90, Br80].

(continued on next page)

Table 2 (continued)

63 Eu	IS for Eu I; $\delta\langle r^2 \rangle$ recalculated using IS ^{(137–139)Eu} [Ba04] and IS ^{(154)Eu} [Zh84] at 576.5 nm ($6s^2\ ^8S_{7/2} \rightarrow 6s6p\ ^6P_{7/2}$) with $F_{se} = -6.55$ GHz/fm ² , $MS_{se} \approx N = +285$ GHz u [Ba04]; IS ^{(140–153)Eu} at 462.7 nm ($4f^7 6s^2\ ^8S_{7/2} \rightarrow 4f^7 6s6p\ ^8P_{7/2}$) with $F_{se} = -5.25$ GHz/fm ² ; $MS_{se} \approx N = +355$ GHz u [Ah85]; IS ^{(155–159)Eu} at 601.8 nm ($6s^2\ ^8S_{7/2} \rightarrow 6s6p\ ^8P_{9/2}$) with $F_{se} = -6.57$ GHz/fm ² , $MS_{se} \approx N = +274$ GHz u [Al90].
64 Gd	IS of Gd I; $\delta\langle r^2 \rangle$ recalculated using IS ^{(146–160)Gd} projected values on 585.2 nm ($5d6s^2\ ^9D_5 \rightarrow 5d6s6p\ ^9D_5$) – see [14] and references therein; $F_{se} = -7.08$ GHz/fm ² , $MS_{se} = +167(139)$ GHz u [Bo87, Al88]; IS ^{(145,160)Gd} at 569.6 nm ($5d6s^2\ ^9D_4 \rightarrow 5d6s6p\ ^9D_5$), $F_{se} = -7.03$ GHz/fm ² , $MS_{se} = +162(139)$ GHz u [Ba05, Bo87].
65 Tb	IS for Tb I at 579.6 nm ($4f^9 6s^2\ ^6H \rightarrow 4f^9 6s6p\ H_{17/2}$); $F_{se} = -7.83$ GHz/fm ² , $MS_{se} \approx N = +283.7$ GHz u [Al90b].
66 Dy	Data for radioactive isotopes are not published; $\delta\langle r^2 \rangle$ recalculated using λ as given by [5]; IS for Dy I at 421 nm (D_1 -line) $F_{se} = -7.26$ GHz/fm ² , $MS_{se} \approx N = +390$ GHz u [5] (see also the references therein); in this case the uncertainties include statistical and systematic errors.
67 Ho	IS for Ho I at 592.2 nm ($4f^{11} 6s^2\ ^4I_{15/2} \rightarrow 4f^{11} 6s6p\ (15/2, 1)_{15/2}$ transition), $F_{se} = -8.41$ GHz/fm ² , $MS_{se} \approx N = +278$ GHz u [Al89]; IS ^{(151)Ho} not published; the $\lambda^{165,151}$ given in [5] was used.
68 Er	IS for Er I – projected values on 582.7 nm ($4f^{12} 6s^2\ ^3H_6 \rightarrow [4f^{12} 6s6p\ (^3P_1)]_7$) – (see [14] and references therein); $\delta\langle r^2 \rangle$ recalculated with $F_{se} = -8.08$ GHz/fm ² , $MS_{se} \approx N = +282$ GHz u (preliminary values of [5, Ne84]).
69 Tm	IS for Tm I at 597.13 nm ($4f^{13} 6s^2\ ^2F_{7/2} \rightarrow 4f^{13} 6s6p\ ^2P_{7/2}$); IS ^{(153,154)Tm} [Ba00]; IS ^{(156)Tm} [Al87]; IS ^{(157–172)Tm} [Al88b] nm; $\delta\langle r^2 \rangle$ recalculated with $F_{se} = -10.3$ GHz/fm ² , $MS_{se} \approx N = +275$ GHz u [Al88b].
70 Yb	Yb I; $\delta\langle r^2 \rangle$ recalculated using IS ^{(152–176)Yb} projected values on 555.6 nm ($4f^{14} 6s^2\ ^1S_0 \rightarrow 4f^{14} 6s6p\ ^3P_1$) (see [14] and references therein) with $F_{se} = -11.5$ GHz/fm ² , $MS_{se} = +4581(1531)$ GHz u from combined optical, muonic and electronic K _x data analysis of [Cl79].
71 Lu	IS for Lu I at 451.9 nm ($5d6s^2\ ^2D_3 \rightarrow 5d6s6p\ ^2D_3$) [Ge98]; $\delta\langle r^2 \rangle$ recalculated relative 175 Lu with $F_{se} = -11.2$ GHz/fm ² , $MS_{se} \approx N = +362$ GHz u from [Ge98] with HM correction as given in [14].
72 Hf	Hf II; $\delta\langle r^2 \rangle^{170–175, 176–182}$ recalculated using IS projected values on 301.3 nm ($5d6s^2\ ^2D_{3/2} \rightarrow 5d6s6p\ ^2D_{5/2}$) – (see [14] and references therein) with $F_{se} = -22.1(4)$ GHz/fm ² , $MS_{se} = +298(503)$ GHz u using analysis of [Zi94, Le99]; IS ^{(171)Hf} at 301.3 nm from [Ye00]; $\delta\langle r^2 \rangle^{174, 175}$ from [Ji97].
74 W	$\delta\langle r^2 \rangle$ mean value of four optical transition of W I; reference transition 543.5 nm ($5d^4 6s^2\ ^5D_1 \rightarrow 5d^4 6s6p\ ^7F_1$); $F_{se} = +19.85$ GHz/fm ² , $MS_{se} \approx N = +303(152)$ GHz u [Ji94].
75 Re	$\lambda^{187, 185}$ from [Kr86] additionally corrected for HM.
76 Os	$\lambda^{A/A}$ of [Au87] (see also the references therein) corrected for HM.
77 Ir	IS for Ir I at 351.5 nm ($5d^7 6s^2\ ^4F_9 \rightarrow 5d^7 6s6p\ ^6F_{11/2}$); $\delta\langle r^2 \rangle$ from [Ve06]; $F_{se} = -30.94$ GHz/fm ² , $MS_{se} \approx N = +468(234)$ GHz u.
78 Pt	IS ^{(183–198)Pt} for Pt I at 265.57 nm ($5d^9 6s\ ^3D_3 \rightarrow 5d^9 6p\ ^7P_4$) [Hi92], $F_{se} = -20.78$ GHz/fm ² , $MS_{se} = +798$ GHz u; IS ^{(178–185)Pt} for Pt I at 306.5 nm ($5d^9 6s\ ^3D_3 \rightarrow 5d^9 6p\ ^3P_2$), [Bl00, Sa00], $F_{se} = -18.5(10)$ GHz/fm ² , $MS_{se} = +764$ GHz u via King plot for stable Pt isotopes using [Ne87].
79 Au	IS for Au I, projected values on 267.6 nm ($5d^{10} 6s\ ^2S_{1/2} \rightarrow 5d^{10} 6p\ ^2P_{1/2}$) [14] (see also references therein) for ^{184–189} Au; ¹⁸³ Au at 267.6 nm [Kr88]; $F_{cal} = -43.07$ GHz/fm ² , $MS_{se} = +799(553)$ GHz u [Wa87, Pa94].
80 Hg	IS ^{(181–204)Hg} for Hg I projected values on 253.65 nm ($5d^{10} 6s^2\ ^3S_0 \rightarrow 5d^{10} 6s6p\ ^3P_1$) (see [14] and references therein); IS ^{(205,206)Hg} [Ul86]; $\delta\langle r^2 \rangle$ recalculated with $F_{cal} = -55.36$ GHz/fm ² [To85], $MS_{se} \approx N = +648(324)$ GHz u. IS ^{(190–207)Hg} projected values on 535 nm ($6s^2 6p\ ^2P_{3/2} \rightarrow 6s^2 7s\ ^2S_{1/2}$) [14] (see also references therein).
81 Tl	IS ^{(188)Tl} for Tl I at 535 nm ($6s^2 6p\ ^2P_{3/2} \rightarrow 6s^2 7s\ ^2S_{1/2}$) from [Me92]; $\delta\langle r^2 \rangle$ recalculated with $F_{cal} = +18.94$ GHz/fm ² [Me92], $MS_{se} \approx +399(83)$ GHz u; $\delta\langle r^2 \rangle^{207, 208}$ [La92] recalculated relative ²⁰⁵ Tl using IS ^{(205,207)Tl} at 535 nm [Ne85].
82 Pb	IS for Pb I on 283.3 nm ($6s^2 6p^2\ ^3P_0 \rightarrow 6s^2 6p7s\ ^3P_1$); IS ^{(196–214)Pb} [An86b]; IS ^{(182–189)Pb} [Wi07, Se09]; IS ^{(190–195)Pb} projected values on 283.3 nm [14], $F_{e\mu} = +20.26(18)$ GHz/fm ² [An86b], $MS_{cal} = +0.19(25) \cdot N = +110(145)$ GHz u [Ki85].
83 Bi	IS for Bi I at 306.7 nm ($6s^2 6p^3\ ^4S_{3/2} \rightarrow 6s^2 6p^2 7s\ ^4P_{1/2}$) [Pe00]; $\delta\langle r^2 \rangle$ estimated using experimental value of $\delta\langle r^2 \rangle^{208, 206} = -0.119$ fm ² $\approx \langle r^2 \rangle^{209, 207}$ with an adopted uncertainty of 0.020 fm ² ; $F_{est} = -25.4(4.3)$ GHz/fm ² and $MS_{se} \approx N = +536$ GHz u.
84 Po	Po I at $\lambda = 843.38$ nm ($6p^3 7s\ ^5S_2 \rightarrow 6p^3 7p\ ^5P_2$) – even isotopes [Co11]; IS(odd isotopes) [Ko91] projected values on 843.38 nm; $F_{cal} = -12.786$ GHz/fm ² ; $MS_{cal} = -116$ GHz u [Co10].
86 Rn	IS for Rn I at 745 nm, $7s[3/2]_2 \rightarrow 7p[5/2]_3$ transition (see Fig. 3 [Bo87b]), $\delta\langle r^2 \rangle$ recalculated using $F_{se} = -22.1$ GHz/fm ² [5], $MS_{se} \approx N = +221$ GHz u.
87 Fr	IS for Fr I at 717.97 nm, D_2 -line [Co85]; $\delta\langle r^2 \rangle$ recalculated in [Co87] with $F_{se} = -24.10$ GHz/fm ² , $MS_{se} \approx N = +229$ GHz u.
88 Ra	IS for Ra I at 482.6 nm, $7s^2\ ^1S_0 \rightarrow 7s7p\ ^1P_1$ transition; $\delta\langle r^2 \rangle$ as given by [Ah88]; $F_{se} = -35.27$ GHz/fm, $MS_{se} \approx N = +341$ GHz u (see [We87, Ah88]).
90 Th	IS for Th II at 583.89 nm ($6d^2 7s\ ^4F_{3/2} \rightarrow 5f6d^2$); $\delta\langle r^2 \rangle$ as given by [Kä89] with statistical errors only, $F_{phen} = -81.3(11.2)$ GHz/fm ² , calibrated using $\lambda^{232, 230} = 0.189(26)$ fm ² (see [Au87] and references therein), $MS_{se} \approx N = +282$ GHz u.
92 U	IS for U I at 591.5 nm ($6d7s^2\ ^5L_0 \rightarrow 6d7s7p\ ^7M_7$) [An92]; $F_{phen} = -33.6(7.4)$ GHz/fm ² , calibrated using $\lambda^{238, 236} = -0.151(34)$ fm ² (see [Au87] and references therein), $MS_{se} \approx N = +278$ GHz u.
94 Pu	IS for Pu I at 420.64 nm ($f^6 s^2 \rightarrow f^6 sp$) [Ge87]; $\delta\langle r^2 \rangle$ recalculated assuming $MS_{se} \approx N = +391$ GHz u, $F = -42.4(3.6)$ GHz/fm ² obtained by one parameter fit to model dependent muonic radii of ^{239, 240, 242} Pu of [Zu86] (see also [14]).
95 Am	$\lambda^{243, 241} = -0.128(7)$ [Ba98] (see references therein) corrected for HM.
96 Cm	$\lambda^{244, A}$ from [Au87] (see references therein) corrected for HM.

References for Table 2 (for radii changes from OIS).

- [Ki64] W.H. King, *Isotope shifts in the arc spectrum of ruthenium*, Proc. Roy. Soc. London 280 (1964) 430.
- [Fi74] W. Fischer, H. Hühnermann, K. Mandrek, *Isotope shift measurements in the atomic spectrum of lanthanum*, Z. Phys. 269 (1974) 245.
- [He74] K. Heilig, A. Steudel, At. Data Nucl. Data Tables 14 (1974) 613.
- [Be79] K. Bekk, A. Andle, S. Göring, A. Hansel, G. Nowicki, H. Rebel, G. Schatz, *Laserspectroscopic study of collective properties of neutron deficient Ba nuclei*, Z. Phys. A 291 (1979) 219.
- [Cl79] D.L. Clark, M.E. Cage, D.A. Lewis, G.W. Greenlees, *Optical isotope shifts and hyperfine splittings for Yb*, Phys. Rev. 20 (1979) 239.
- [Br80] H. Brand, B. Seibert, A. Steudel, *Laser-atomic-beam spectroscopy in Sm: isotope shifts and changes in mean-square charge radii*, Z. Phys. A 296 (1980) 281.
- [St80] A. Steudel, U. Triebe and D. Wendtlandt, *Isotope shift in Ni I and changes in mean square nuclear charge radii of stable Ni isotopes*, Z. Phys. A 296 (1980) 189.
- [Wo81] H.D. Wohlfahrt, E.B. Shera, M.V. Hoehn, Y. Yamazaki, R.M. Steffen, *Nuclear charge distributions in $^{1}f_{7/2}$ -shell nuclei from muonic X-ray measurements*, Phys. Rev. C 23 (1981) 523.
- [Th81] C. Thibault, F. Touchard, S. Büttgenbach, R. Klapisch, M. de Saint Simon, H.T. Duong, P. Jaquinot, P. Juncar, S. Liberman, P. Pillet, J. Pinard, J.L. Vialle, A. Pesnelle, G. Hube, *Hyperfine structure and isotope shift of the D_2 line of $^{76-98}\text{Rb}$ and some their isomers*, Phys. Rev. C 23 (1981) 2720.
- [Th81b] C. Thibault, F. Touchard, S. Büttgenbach, R. Klapisch, M. de Saint Simon, H.T. Duong, P. Jaquinot, P. Juncar, S. Liberman, P. Pillet, J. Pinard, J. L. Vialle, A. Pesnelle, G. Huber, *Hyperfine structure and isotope shift of the D_2 line of $^{118-145}\text{Cs}$ and some their isomers*, Nuclear Phys. A 367 (1981) 1.
- [Hu82] G. Huber, F. Touchard, S. Büttgenbach, C. Thibault, R. Klapisch, H.T. Duong, S. Liberman, J. Pinard, J.L. Vialle, P. Juncar, P. Jaquinot, *Spin, magnetic moments and isotope shifts of $^{21-31}\text{Na}$ by high resolution laser spectroscopy of the atomic D_1 line*, Phys. Rev. C 18 (1978) 2342.
- [To82] F. Touchard, P. Guimbal, S. Büttgenbach, R. Klapisch, M. de Saint Simon, C. Thibault, H.T. Duong, P. Juncar, S. Lieberman, J. Pinard, J.L. Vialle, *Isotope shifts and hyperfine structure of $^{37-48}\text{K}$ by laser spectroscopy*, Phys. Lett. B 108 (1982) 169.
- [Ba83] P. E.G. Baird, S.A. Blundell, G. Burrows, C. J. Foot, G. Meiselt, D.N. Stacey, G. K. Woodgate, *Laser spectroscopy of the tin isotopes*, J. Phys. B: At. Mol. Phys. 16 (1983) 2485.
- [Ma84] G.K. Mallot: Ph.D.Thesis, Univ. Mainz (1984).
- [Ne84] R. Neugart, private communication.
- [Pa84] C.W.P. Palmer, P.E.G. Baird, S.A. Blundell, J.R. Brandenberger, C.J. Foot, D.N. Stacey, G.W. Woodgate, *Laser spectroscopy of calcium isotopes*, J. Phys. B: At. Mol. Phys. 17 (1984) 2197.
- [Zh84] A.N. Zherikhin, O.N. Kompanets, V.S. Letokhov, I.V. Mishin, V.N. Fedoseev, G.D. Alkhasov, A.E. Barzakh, E.E. Berlovich, V.P. Denisov, A.G. Dernatian, V.S. Ivanov, *High-resolution laser photoionization spectroscopy of radioactive europium isotopes*, Zh. Eksp. Teor. Fiz. 86 (1984) 1249.
- [Ah85] S.A. Ahmad, W. Klempt, C. Eksröm, R. Neugart, K. Wendt, *Nuclear spins, moments and changes of the mean square radii of $^{140-153}\text{Eu}$* , Z. Phys. A 321 (1985) 35.
- [Bl85] S.A. Blundell, P.E.G. Baird, C.W.P. Palmer, D.N. Stacey, G.K. Woodgate, D. Zimmermann: A Re-Evaluation of Isotope Shift Constants, Z. Physik A - Atoms and Nuclei 321 (1985) 31.
- [Co85] A.Coc, C. Thibault, F. Touchard, H.T. Duong, P. Juncar, S. Liberman, J. Pinard, J. L. L. Vialle, S. Büttgenbach, A.C. Mueller, A. Pesnelle and the ISOLDE Collaboration, *Hyperfine structure and isotope shifts of $^{207-213,220-228}\text{Fr}$: possible evidence of octupole deformation*, Phys. Lett. 163B (1985) 66.
- [Ki85] W.H. King, M. Wilson, *Isotope shifts in lead: mass shifts and the odd-even effect*, J. of Phys. G 11 (1985) L43.
- [Ne85] R. Neugart, H.H. Stroke, S.A. Ahmad, H.T. Duong, H.L. Ravn, K. Wendt, *Nuclear magnetic moment of ^{207}Tl* , Phys. Rev. Lett. 55 (1985) 1559.
- [To85] G. Torbohm, G. Fricke, A. Rosén, *State dependent volume isotope shifts of low lying states of group IIa and IIb elements*, Phys. Rev. A 31 (1985) 2038.
- [An86] M. Anselment, K. Bekk, A. Hanser, H. Hoeffgen, G. Meisel, S. Göring, H. Rebel, G. Schatz, *Charge radii and moments of tin nuclei by laser spectroscopy*, Phys. Rev. C 34 (1986) 1052.
- [An86b] M. Anselment, W. Faubel, S. Göring, A. Hansen, G. Meisel, H. Rebel, G. Schatz, *The odd-even staggering of the nuclear charge radii of Pb isotopes*, Nuclear Phys. A 451 (1986) 471.
- [Kr86] J.-R. Kropp, H.-D. Kronfeldt, A. Lucas, R. Winkler, *Isotope shift and hyperfine-structure analysis in the Re I configurations (5d + 6s) 66p*, Physica B + C 138 (1986) 335.
- [Ul86] G. Ulm, S.K. Bhattacharjee, P. Dabkewicz, G. Huber, H.-J. Kluge, T. Kiihl, H. Lochmann, E.-W. Otten, K. Wendt, A.A. Ahmad, W. Klempt, R. Neugart and the ISOLDE Collaboration, *Isotope shift of ^{182}Hg and update of nuclear moments and charge radii in the isotope range ^{181}Hg – ^{206}Hg* , Z. Phys. A 325 (1986) 247.
- [Zu86] J.D. Zumbro, R.A. Naumann, M.V. Hoehn W. Reuter, E. B. Shera, C. E. Bemis, Jr., Y. Tanaka, *E2 and E4 deformations in ^{232}Th and $^{239,240,242}\text{Pu}$* , Phys. Lett. B 167 (1986) 383.
- [Al87] G.D. Alkhazov, A.E. Barzakh, V.N. Buyanov, V.P. Denisov, V.S. Ivanov, V.S. Letokhov, V.I. Mishin, S.K. Sekatsky, V.N. Fedoseyev, I.Y. Chubukov, *Studies of nuclear charge radii and electromagnetic moments of radioactive Nd, Sm, Eu, Ho, Tm isotopes by laser resonance atomic photoionization technique*, Preprint 1309. INP of the Acad. Sci. USSR, Leningrad, 1987.
- [Au87] P. Aufmuth, K. Heilig, A. Steudel, *Mean-square nuclear charge radii from optical isotope shifts*, At. Data Nucl. Data Tables 87 (1987) 455.
- [Bo87] S. K. Borisov, Yu.P. Gangrsky, C. Hradecny, S.G. Zemlyanoi, B.B. Krynetsky, K.P. Marinova, B.N. Markov, V.A. Mishin, Yu.Ts. Oganessian, O.M. Stel'makh, Hoang Thi Kim Hue, Tran Cong Tam, *Measurements of the charge radii changes of Nd, Sm and Gd nuclides by resonance laser light*, Sov. Phys. JETP 66 (1987) 882.
- [Bo87b] W. Borchers, R. Neugart, E.W. Otten, H.T. Duong, G. Ulm, K. Wendt, *Hyperfine structure and isotope shifts investigations in $^{202-222}\text{Rn}$ for the study of nuclear structure beyond $Z = 82$* , Hyperfine Interact. 34 (1987) 25.
- [Co87] A.Coc, C. Thibault, F. Touchard, H.T. Duong, P. Juncar, S. Liberman, J. Pinard, M. Carre, J. L. L. Vialle, S. Büttgenbach, A.C. Mueller, A. Pesnelle, *Isotope shift, spin and hyperfine structure of $^{118,146}\text{Cs}$ and some francium isotopes*, Nuclear Phys. A 468 (1987) 1.
- [Eb87] J. Eberz, U. Dinger, G. Huber, H. Lochmann, R. Menges, R. Neugart, R. Kirchner, O. Klepper, T.U. Kiihl, D. Marx, G. Ulm, K. Wendt, *Spins, moments and mean square charge radii of $^{104-127}\text{In}$ determined by laser spectroscopy*, Nuclear Phys. A 464 (1987) 9.
- [Eb87b] J. Eberz, U. Dinger, G. Huber, H. Lochmann, R. Menges, G. G. Ulm, R. Kirchner, O. Klepper, T.U. Kiihl, D. Marx, *Nuclear spins, moments and charge radii of $^{108-111}\text{Sn}$* , Z. Phys. A 326 (1987) 121.
- [Ge87] S. Gesterinkorn, F. Tomkins, *Evaluation de l'effet spécifique de masse dans le spectre d'arc du plutonium*, Phys. Scr. 36 (1987) 240.
- [Ne87] W. Neu, G. Passler, G. Sawatzky, R. Winkler, H.-J. Kluge, *Isotope shift and hyperfine structure of stable platinum isotopes*, Z. Phys. D 7 (1987) 193.
- [Wa87] K. Walmeroth, G. Bollen, A. Dohn, P. Egelhof, J. Grüner, F. Lindenlauf, U. Krönert, J. Campos, A. Rodriguez Yunta, M.J.G. Borge, A. Venugopalan, J.L. Wood, R. B. Moor, H.-J. Kluge, *Sudden change in the nuclear charge distribution of very light gold isotopes*, Phys. Rev. Lett. 58 (1987) 1516.
- [We87] K. Wendt, S.A. Ahmad, W. Klempt, R. Neugart, E.W. Otten, H.H. Stroke, *On the hyperfine structure and isotope shift of radium*, Z. Phys. D 4 (1987) 227.

- [Ah88] S.A. Ahmad, W. Klempt, R. Neugart, E.W. Otten, P.-G. Reinhard, G. Ulm, K. Wendt, *Mean square charge radii of radium isotopes and octupole deformation in the $^{220-228}\text{Ra}$ region*, Nuclear Phys. A 483 (1988) 224.
- [Al88] G.D. Alkhazov, A.E. Barzakh, V.P. Denisov, V.S. Ivanov, I.Y. Chubukov, N.B. Buyanov, V.S. Letokhov, V.I. Mishin, S.K. Sekatskii, V.N. Fedoseev, *Isotopic changes of gadolinium nuclei charge radii and magic nucleus charge radius ^{146}Gd* , Akad. Nauk USSR, Leningrad Inst. Yad. Fis., preprint No 1417, 20 pages (1988); (in Russian); *Mean square charge radius of the magic nucleus ^{146}Gd* , Zh. Eksp. Theor. Fiz. 48 (1988) 373.
- [Al88b] G.D. Alkhazov, A.E. Barzakh, I.Y. Chubukov, V.P. Denisov, V.S. Ivanov, V.N. Panteleev, V.E. Starodubsky, N.B. Buyanov, M.N. Fedoseyev, V.S. Letokhov, V.I. Mishin, S.K. Sekatskii, *Nuclear electromagnetic moments and charge radii of deformed thulium isotopes with the mass numbers $A = 157-172$* , Nuclear Phys. A 477 (1988) 37.
- [Kr88] U. Krönert, S. Becker, G. Bollen, M. Gerber, T. Hilberath, H.-J. Kluge, G. Passler and the ISOLDE Collaboration, *Observation of strongly deformed ground state configuration in ^{184}Au and ^{187}Au by laser spectroscopy*, Z. Phys. A 331 (1988) 521.
- [Al89] G.D. Alkhazov, A.E. Barzakh, I.Y. Chubukov, V.P. Denisov, V.S. Ivanov, N.B. Buyanov, *Nuclear deformation of holmium isotopes*, Nuclear Phys. A 504 (1989) 549.
- [Bo89] W. Borchers, E. Arnold, W. Neu, R. Neugart, K. Wendt, G. Ulm and ISOLDE Collaboration, *Xenon isotopes far from stability studied by collisional ionization laser spectroscopy*, Phys. Lett. B 216 (1989) 7.
- [Di89] U. Dinger, J. Eberz, G. Huber, R. Menges, R. Kirchner, O. Klepper, T. Kühl, D. Marx, *Nuclear moments and change in the charge radii of neutron-deficient silver isotopes*, Nuclear Phys. A 503 (1989) 331.
- [Kä89] W. Kälber, J. Ring, W. Faubel, S. Göring, G. Meisel, H. Rebel, R.C. Thompson, *Nuclear radii of thorium isotopes from laser spectroscopy*, Z. Physics A334, (1989) 103.
- [Ot89] E.W. Otten, *Nuclear radii and moments of unstable isotopes*, in Treatise on heavy-ion science, D.A. Bromley, Editor. 1989. p. 517–638.
- [Al90] G.D. Alkhazov, A.E. Barzakh, V.A. Bolshakov, V.P. Denisov, V.S. Ivanov, Y.Y. Sergeyev, I.Y. Chubukov, V.I. Tikhonov, V.S. Letokhov, V.I. Mishin, S.K. Sekatsky, V.N. Fedoseyev, *Odd–even staggering in nuclear charge radii of neutron-rich europium isotopes*, Z. Phys. A 337 (1990) 257.
- [Al90b] G.D. Alkhazov, A.E. Barzakh, V.P. Denisov, V.S. Ivanov, I.Y. Chubukov, V.S. Letokhov, V.I. Mishin, S.K. Sekatsky, V.N. Fedoseyev, *Electromagnetic moments and nuclear charge radii for neutron-deficient Tb isotopes and the deformation jump near $Z = 64$, $N = 90$* , Z. Phys. A 337 (1990) 367.
- [Bu90] F. Buchinger, E.B. Ramsay, E. Arnold, W. Neu, R. Neugart, K. Wendt, R.E. Silverans, P. Lievens, L. Vermeeren, D. Berdichevsky, R. Fleming, D.W.L. Sprung, G. Ulm, *Systematics of nuclear ground state properties in $^{78-100}\text{Sr}$ by laser spectroscopy*, Phys. Rev. C 41 (1990) 2883.
- [En90] J.G. Englandt, I.S. Grant, J.A.R. Griffith, D.E. Evans, D.A. Eastham, G.W.A. Newton, P.M. Walker, *Isotope shifts and hyperfine splittings in $^{144-151}\text{Sm}$* , J. Phys. G 16 (1990) 105.
- [Pi90] C. Piller, C. Gugler, R. Jacot-Guillarmod, L.A. Schaller, L. Schellenberg, H. Schneuwly, G. Fricke, T. Hennemamm, J. Herzberz, *Nuclear charge radii of the tin isotopes from muonic atoms*, Phys. Rev. C 42 (1990) 182.
- [Ko91] D. Kowalewska, K. Bekk, S. Göring, A. Hanser, W. Kälber, G. Meisel, H. Rebel, *Isotope shifts and hyperfine structure in polonium isotopes by atomic-beam laser spectroscopy*, Phys. Rev. A 44 (1991) R1442.
- [Li91] P. Lievens, R.E. Silverans, L. Vermeeren, W. Borchers, W. Neu, R. Neugart, K. Wendt, F. Buchinger, E. Arnold and ISOLDE. Collaboration, *Nuclear ground state properties of ^{99}Sr by collinear laser spectroscopy with non-optical detection*, Phys. Lett. B 256 (1991) 141.
- [An92] A. Anastasov, Yu.P. Gangrsky, K.P. Marinova, B.N. Markov and S.G. Zemlyanoi, *Nuclear charge radii changes of uranium and hafnium isotopes determined by laser spectroscopy*, Hyperfine Interact. 74 (1992) 31.
- [Hi92] T. Hilberath, S. Becker, G. Bollen, H.-J. Kluge, U. Krönert, G. Passler, J. Rikovska, R. Wyss and ISOLDE Collaboration, *Ground-state properties of neutron-deficient platinum isotopes*, Z. Phys. A 342 (1992) 1.
- [La92] W. Lauth, H. Backe, M. Dahlinger, I. Kluft, P. Schwamb, G. Schwickert, N. Trautmann, U. Othmer, *Resonance ionization spectroscopy in a buffer gas cell with radioactive decay detection, demonstrated using ^{208}Tl* , Phys. Rev. Lett. 68 (1992) 1675.
- [Le92] V.S. Letokhov, V.I. Mishin, S.K. Sekatsky, V.N. Fedoseyev, G.D. Alkhazov, A.E. Barzakh, V.P. Denisov, V.E. Starodubsky, *Laser spectroscopic studies of nuclei with neutron number $N < 82$ (Eu, Sm and Nd isotopes)*, J. Phys. G 18 (1992) 1177.
- [Li92] P. Lievens, L. Vermeeren, R.E. Silverans, E. Arnold, R. Neugart, K. Wendt, F. Buchinger, *Spin, moments, and mean square nuclear charge radius of $^{77-88}\text{Sr}$* , Phys. Rev. C 46 (1992) 797.
- [Mä92] A.-M. Mårtensson-Pendrill, A. Ynnerman, H. Warston, L. Vermeeren, R.E. Silverans, A. Klein, R. Neugart, C. Schulz, P. Lievens, *Isotope shifts and nuclear-charge radii in singly ionized $^{40-48}\text{Ca}$* , Phys. Rev. A 45 (1992) 4675.
- [Me92] R. Menges, U. Dinger, N. Boos, G. Huber, S. Schröder, S. Dutta, R. Kirchner, O. Klepper, T. Kühl, D. Marx, G.D. Sprouse, *Nuclear moments and the change in the mean square charge radius of neutron deficient thallium isotopes*, Z. Phys. A 341 (1992) 475.
- [Ve92] L. Vermeeren, R.E. Silverans, P. Lievens, A. Klein, R. Neugart, C. Schulz, F. Buchinger, *Ultrasensitive radioactive detection of collinear-laser optical pumping: Measurement of the nuclear charge radius of ^{50}Ca* , Phys. Rev. Lett. 68 (1992) 1679.
- [Kü93] E. Kümmel, M. Baumann, C.S. Kischkel, *Hyperfine structure and isotope shift in the $4d^9 5s$ configuration of Pd I*, Z. Phys. D 25 (1993) 161.
- [Ji94] W.G. Jin, M. Wakasugi, T.T. Inamura, T. Murayama, T. Wakui, H. Katsuragawa, T. Ariga, T. Ishizuka, M. Koizumi, I. Sugai, *Isotope shifts and hyperfine structure in LuI and W I*, Phys. Rev. A 49 (1994) 762.
- [Ke94] M. Keim, E. Arnold, W. Borchers, U. Georg, A. Klein, R. Neugart, L. Vermeeren, R.E. Silverans, P. Lievens, *Laser-spectroscopy measurements of $^{72-96}\text{Kr}$ spins, moments and charge radii*, Nuclear Phys. A 586 (1994) 219.
- [Pa94] G. Passler, J. Rikovska, E. Arnold, H.-J. Kluge, L. Monz, R. Neugart, H. Ravn, K. Wendt and ISOLDE Collaboration, *Quadrupole moments and nuclear shape of neutron-deficient gold isotopes*, Nuclear Phys. A580 (1994) 173.
- [Zi94] D. Zimmermann, P. Baumann, D. Kuszner, A. Werner, *Isotope shift and hyperfine structure in atomic spectrum of hafnium by laser spectroscopy*, Phys. Rev. A 50 (1994) 1112.
- [KI96] A. Klein, B.A. Brown, U. Georg, M. Keim, P. Lievens, R. Neugart, M. Neuroth, R.E. Silverans, L. Vermeeren, and ISOLDE Collaboration, *Moments and mean square charge radii of short-lived argon isotopes*, Nuclear Phys. A 607 (1996) 1.
- [Ve96] L. Vermeeren, P. Lievens, R.E. Silverans, U. Georg, M. Keim, A. Klein, R. Neugart, M. Neuroth, F. Buchinger, and ISOLDE Collaboration, *The mean square nuclear charge radius of ^{39}Ca* , J. Phys. G 22 (1996) 1517.
- [Be97] D. M. Bentley, E.C.A. Cochrane, J.A.R. Griffith, *Optical isotope shifts in the iron atom*, J. Phys. B: At. Mol. Opt. Phys. 30 (1997) 5359.
- [Ca97] P. Campbell, J. Billowes, I. S. Grant, *The specific mass shift of the zinc atomic ground state*, J. Phys. B: At. Mol. Opt. Phys. 30 (1997) 2351.
- [Ji97] W. G. Jin, M. Wakasugi, M. G. Hies, T. T. Inamura, T. Murayama, T. Ariga, A. Yamashita, T. Wakui, H. Katsuragawa, T. Ishizuka, J. Z. Ruan, I. Sugai, *Nuclear moments and charge radius of ^{175}Hf from optical measurement of hyperfine structure*, Phys. Rev. C 55 (1997) 1545.
- [Ba98] H. Backe, M. Hies, H. Kunz, W. Lauth, O. Curtze, P. Schwamb, M. Sewtz, W. Theobald, R. Zahn, K. Eberhardt, N. Trautmann, D. Habs, R. Repnow, B. Fricke, *Isotope Shift Measurements for Superdeformed Fission Isomeric States*, Phys. Rev. Lett. 80 (1998) 920.
- [Ge98] U. Georg, W. Borchers, M. Keim, A. Klein, P. Lievens, R. Neugart, M. Neuroth, P.M. Rao, C. Schulz and ISOLDE Collaboration, *Laser spectroscopy investigation of the nuclear moments and radii of lutetium isotopes*, Eur. Phys. J. A 3 (1998) 225.

- [Le99] J. M. G. Levis, D. M. Benton, J. Billowes, P. Campbell, T. G. Cooper, P. Dendooven, D. E. Evans, D. H. Forest, I. S. Grant, J. A. R. Griffith, J. Huikari, A. Jokinen, K. Peräjärvi, G. Tungate, G. Yeandle, J. Äystö, *First On-Line Laser Spectroscopy of Radioisotopes of a Refractory Element*, Phys. Rev. Lett. 82 (1999) 2476.
- [Ba00] A. E. Barzakh, I. Ya. Chubukov, D. V. Fedorov, V. N. Pantelev, M. D. Seliverstov, Yu. M. Volkov, *Mean square charge radii of the neutron-deficient rare-earth isotopes in the region of the nuclear shell $N = 82$ measured by the laser ion source spectroscopy technique*, Phys. Rev. C 61 (2000) 034304.
- [Bl00] F. Le Blanc, The COMPLIS experiment on neutron-deficient Au, Pt and Ir isotopes, Hyperfine Interact. 127 (2000) 71.
- [Pe00] M.R. Pearson, P. Campbell, K. Leerunnavarat, J. Billowes, I.S. Grant, M. Keim, J. Kilgallon, I.D. Moore, R. Neugart, M. Neuroth, S. Wilbert and ISOLDE Collaboration, *Nuclear moments and charge radii of bismuth isotopes*, J. Phys. G 26 (2000) 1829.
- [Sa00] J. Sauvage, N. Boos, L. Cabaret, J.E. Crawford, H.T. Duong, J. Genevey, M. Girod, G. Huber, F. Ibrahim, M. Krieg, F.L. Blanc, J.K.P. Lee, J. Libert, D. Lunney, J. Obert, J. Oms, S. Péru, J. Pinard, J.C. Putaux, B. Roussi re, V. Sebastian, D. Verney, S. Zemlyanoi, J. Arianer, N. Barr , M. Ducourtieux, D. Forkel-Wirth, G.L. Scornet, J. Lettry, C. Richard-Serre, C. V ron. COMPLIS experiments: Collaboration for spectroscopy, *Measurements using a Pulsed Laser Ion Source*, Hyperfine Interact. 129 (2000) 303.
- [Ye00] G. Yeandle, J. Billowes, P. Campbell, E.C.A. Cochrane, P. Dendooven, D.E. Evans, J.A.R. Griffith, J. Huikari, A. Jokinen, I.D. Moore, A. Nieminen, K. Per  jarvi, G. Tungate, J.   yst , *Nuclear moments and charge radii of the ^{171}Hf ground state and isomer*, J. Phys. G 26 (2000) 839.
- [Ca02] P. Campbell, H.L. Thayer, J. Billowes, P. Dendooven, K.T. Flanagan, D.H. Forest, J.A.R. Griffith, J. Huikari, A. Jokinen, R. Moore, A. Nieminen, G. Tungate, S. Zemlyanoi, J.   yst , *Laser Spectroscopy of Cooled Zirconium Fission Fragments*, Phys. Rev. Lett. 89 (2002) 082501.
- [Fo02] D.H. Forest, J. Billowes, P. Campbell, P. Dendooven, K.T. Flanagan, J.A.R. Griffith, J. Huikari, A. Jokinen, R. Moore, A. Nieminen, H.L. Thayer, G. Tungate, S. Zemlyanoi, J.   yst , *Laser spectroscopy of neutron deficient zirconium isotopes*, J. Phys. G 28 (2002) L63.
- [Ch03] B. Cheal, M. Avgoulea, J. Billowes, P. Campbell, K.T. Flanagan, D.H. Forest, M. D. Gardner, J. Huikari, B.A. Marsh, A. Nieminen, H.L. Thayer, G. Tungate, J.   yst , *Collinear laser spectroscopy of neutron-rich cerium isotopes near the $N = 88$ shape transition*, J. Phys. G 29 (2003) 2479.
- [li03] H. Iimura, M. Koizumi, M. Miyabe, M. Oba, T. Shibata, N. Shinohara, Y. Ishida, T. Horiguchi, H. A. Schuessler, *Nuclear moments and isotope shifts of ^{135}La , ^{137}La , and ^{138}La by collinear laser spectroscopy*, Phys. Rev. C 68 (2003) 054328.
- [Ba04] A.E. Barzakh, D.V. Fedorov, A.M. Ionan, V.S. Ivanov, F.V. Moroz, K.A. Mezilev, S.Yu. Orlov, V.N. Pantelev, Yu.M. Volkov, *Changes in the mean square charge radii of neutron-deficient europium isotopes measured by the laser ion source resonance ionization spectroscopy*, Eur. Phys. J. A 22 (2004) 69.
- [Dr04] G.W.F. Drake, *Helium. Relativity and QED*, Nuclear Phys. A 737 (2004) 25.
- [Ew04] G. Ewald, W. N rtersh user, A. Dax, S. G tte, R. Kirchner, H.-J. Kluge, T. K hl, R. Sanchez, A. Wojtaszek, B.A. Bushaw, G.W.F. Drake, Z.-C. Yan, C. Zimmerman, *Nuclear Charge Radii of $^{8,9}\text{Li}$ Determined by Laser Spectroscopy*, Phys. Rev. Lett. 93 (2004) 113002.
- [Ga04] Yu.P. Gangrsky, K.P. Marinova, S.G. Zemlyanoi, I.D. Moore, J. Billowes, P. Campbell, K.T. Flanagan, D.H. Forest, J.A.R. Griffith, J. Huikari, R. Moore, A. Nieminen, H. Thayer, G. Tungate, J.   yst , *Nuclear charge radii of neutron deficient titanium isotopes ^{44}Ti and ^{45}Ti* , J. Phys. G 30 (2004) 1089.
- [Mu04] P. Mueller, I. A. Sulai, A.C.C. Villari, J.A. Alc ntara-N  ez, R. Alves-Cond , K. Bailey, G.W. F. Drake, M. Dubois, C. El on, G. Gaubert, R. J. Holt, R.V. F. Janssens, N. Lecesne, Z.-T. Lu, T. P. O'Connor, M.-G. Saint-Laurent, J.-C. Thomas, L.-B. Wang, *Nuclear Charge Radius of ^8He* , Phys. Rev. Lett. 99 (2004) 252501.
- [Wa04] L.-B. Wang, P. Mueller, K. Bailey, G.W.F. Drake, J.P. Greene, D. Henderson, R.J. Holt, R.V.F. Janssens, C.L. Jiang, Z.-T. Lu, T.P. O'Connor, R.C. Pardo, K.E. Rehm, J.P. Schiffer, X.D. Tang, *Laser spectroscopic Determination of the ^6He Nuclear Charge Radius*, Phys. Rev. Lett. 93 (2004) 142501.
- [Ba05] A. E. Barzakh, D. V. Fedorov, A. M. Ionan, V. S. Ivanov, F. V. Moroz, K. A. Mezilev, S. Yu. Orlov, V. N. Pantelev, Yu. M. Volkov, *Laser spectroscopic studies of ^{145}Gd , $^{145}\text{Gd}^m$, and $^{143}\text{Gd}^m$* , Phys. Rev. C 72 (2005) 017301.
- [Bl05] F. Le Blanc, L. Cabaret, E. Cott reau, J. E. Crawford, S. Essabaa, J. Genevey, R. Horn, G. Huber, J. Lassen, J. K. P. Lee, G. Le Scornet, J. Lettry, J. Obert, J. Oms, A. Ouchrif, J. Pinard, H. Ravn, B. Roussi re, J. Sauvage, D. Verney, *Charge-radius change and nuclear moments in the heavy tin isotopes from laser spectroscopy: Charge radius of ^{132}Sn* , Phys. Rev. Lett. C 72 (2005) 034305.
- [Ve06] D. Verney, L. Cabaret, J.E. Crawford, H.T. Duong, B. Fricke, J. Genevey, G. Huber, F. Ibrahim, M. Krieg, F. Le Blanc, J.K.P. Lee, G. Le Scornet, D. Lunney, J. Obert, J. Oms, J. Pinard, J.C. Puteaux, K. Rashid, B. Roussi re, J. Sauvage, V. Sebastian and the ISOLDE Collaboration, *Deformation change in light iridium nuclei from laser spectroscopy*, Eur. Phys. J. A 30 (2006) 489.
- [S 06] R. S nchez, W. N rtersh user, A. Dax, G. Ewald, S. G tte, R. Kirchner, H.-J. Kluge, T. K hl, A. Wojtaszek, B.A. Bushaw, G.W. F. Drake, Zong-Chao Yan, C. Zimmermann, D. Albers, J. Behr, P. Bricault, J. Dilling, M. Domsbys, J. Lassen, C. D. P. Levy, M. R. Pearson, E. J. Prime, V. Ryjkov, *Nuclear charge radius of ^{11}Li* , Hyperfine Interact. 171 (2006) 181.
- [S 06b] R. S nchez, W. N rtersh user, G. Ewald, D. Albers, J. Behr, P. Bricault, B. A. Bushaw, A. Dax, J. Dilling, M. Domsbys, G.W. F. Drake, S. G tte, R. Kirchner, H.-J. Kluge, Th. K hl, J. Lassen, C. D. P. Levy, M. R. Pearson, E. J. Prime, V. Ryjkov, A. Wojtaszek, Z.-C. Yan, C. Zimmermann, *Nuclear Charge Radii of ^{9-11}Li : The Influence of Halo Neutron*, Phys. Rev. Lett. 96 (2006) 033002.
- [Ch07] B. Cheal, M. D. Gardner, M. Avgoulea, J. Billowes, M. L. Bissell, P. Campbell, T. Eronen, K. T. Flanagan, D. H. Forest, J. Huikari, A. Jokinen, B. A. Marsh, I. D. Moore, A. Nieminen, H. Penttil , S. Rinta-Antila, B. Tordoff, G. Tungate, J.   yst , *The shape transition in the neutron-rich yttrium isotopes and isomers*, Phys. Rev. Lett. B 645 (2007) 133.
- [Li07] J. Libert, B. Roussi re, J. Sauvage, *Signs of dynamical effects for Cd, Sn, Te, Xe, Ba and Sm nuclear charge radii*, Nuclear Phys. A 786 (2007) 47.
- [Mu07] P. Mueller, I. A. Sulai, A. C. C. Villari, J. A. Alc ntara-N  ez, R. Alves Cond , K. Bailey, G.W. F. Drake, M. Dubois, C. El on, G. Gaubert, R. J. Holt, R.V. F. Janssens, N. Lecesne, Z.-T. Lu, T. P. O'Connor, M.-G. Saint-Laurent, J.-C. Thomas, L.-B. Wang, *Nuclear Charge Radius of ^8He* , Phys. Rev. Lett. 99 (2007) 252501.
- [Wi07] H. de Witte, A. N. Andreyev, N. Barr , M. Bender, T. E. Cocolios, S. Dean, D. Fedorov, V. N. Fedoseyev, L. M. Fraile, S. Franchoo, V. Hellemans, P. H. Heenen, K. Heyde, G. Huber, M. Huyse, H. Jeppensen, U. K ster, P. Kunz, S. R. Leshner, B. A. Marsh, I. Mukha, B. Roussi re, J. Sauvage, M. Seliverstov, I. Stefanescu, E. Tengborn, K. Van de Vel, J. Van de Walle, P. Van Duppen, Yu. Volko., *Nuclear Charge Radii of Neutron-Deficient Lead Isotopes Beyond $N = 104$ Midshell Investigated by In-Source Laser Spectroscopy*, Phys. Rev. Lett. 98 (2007) 112502.
- [Bl08] K. Blaum, W. Geithner, J. Lassen, P. Lievens, K. Marinova, R. Neugart, *Nuclear moments and charge radii of argon isotopes between the neutron-shell closures $N = 20$ and $N = 2$* , Nuclear Phys. A 799 (2008) 30.
- [Ge08] W. Geithner, T. Neff, G. Audi, K. Blaum, P. Delahaye, H. Feldmeier, S. George, C. Gu naut, F. Herfurth, A. Herlert, S. Kappertz, M. Keim, A. Kellerbauer, H.-J. Kluge, M. Kowalska, P. Lievens, D. Lunney, K. Marinova, R. Neugart, L. Schweikhard, S. Wilbert, C. Yazidjian, *Masses and Charge Radii of $^{17-22}\text{Ne}$ and the Two-Proton-Halo Candidate ^{17}Ne* , Phys. Rev. Lett. 101 (2008) 252502.
- [Pu08] M. Puchalski, K. Pachucki, *Relativistic, QED, and finite nuclear mass corrections for low-lying states of Li and Be+*, Phys. Rev. A 78 (2008) 052511.
- [Ya08] Z.-C. Yan, W. N rtersh user, G. W. F. Drake, *High Precision Atomic Theory for Li and Be+: QED Shifts and Isotope Shifts*, Phys. Rev. Lett. 100 (2008) 243002.
- [Ch09] B. Cheal, K. Baczyńska, J. Biliowes, P. Campbell, F.C. Charlwood, T. Eronen, D.H. Forest, T. Kessler, I.D. Moore, M. Reponen, S. Rothe, M. Riiffer, A. Saastamoinen, G. Tungate, J.   yst , *Laser Spectroscopy of Niobium Fission Fragments: First Use of optical Pumping in an Ion Beam Cooler-Buncher*, Phys. Rev. Lett. 102 (2009) 222501.
- [Ch09a] F.C. Charlwood, K. Baczyńska, J. Billowes, P. Campbell, B. Cheal, T. Eronen, D.H. Forest, A. Jokinen, T. Kessler, I.D. Moore, H. Penttil , R. Powis, M. R  ffer, A. Saastamoinen, G. Tungate, J.   yst , *Nuclear charge radii of molybdenum fission fragments*, Phys. Lett. B 674 (2009) 23.

(continued on next page)

- [Nö09] W. Nörtershäuser, D. Tiedemann, M. Žáková, Z. Andjelkovic, K. Blaum, M. L. Bissell, R. Cazan, G.W.F. Drake, Ch. Geppert, M. Kowalska, J. Krämer, A. Krieger, R. Neugart, R. Sánchez, F. Schmidt-Kaler, Z.-C. Yan, D.T. Yordanov, C. Zimmermann, *Nuclear Charge Radii of $^{7,9,10}\text{Be}$ and the One-Neutron Halo Nucleus ^{11}Be* , Phys. Rev. Lett. 102 (2009) 062503.
- [Ro09] B. Roussière, (2009) – private communication
- [Se09] M. D. Seliverstov, A. N. Andreyev, N. Barré, A. E. Barzakh, S. Dean, H. De Witte, D.V. Fedorov, V.N. Fedoseyev, L.M. Fraile, S. Franchoo, J. Genevey, G. Huber, M. Huyse, U. Koester, P. Kunz, S.R. Leshner, B.A. Marsh, I. Mukha, B. Roussière, J. Sauvage, I. Stefanescu, K. Van de Vel, P. Van Duppen, Yu.M. Volkov, *Charge radii and magnetic moments of odd-A $^{183-189}\text{Pb}$ isotopes*, Eur. Phys. J. A 41 (2009) 315.
- [Ch10] F.C. Charlwood, J. Billowes, P. Campbell, B. Cheal, T. Eronen, D.H. Forest, S. Fritzsche, M. Honma, A. Jokinen, I.D. Moore, H. Penttilä, R. Powis, A. Saastamoinen, G. Tungate, J. Aysto, *Ground state properties of manganese isotopes across the $N = 28$ shell closure*, Phys. Lett. B 690 (2010) 346.
- [Pa10] C.G. Parthey, A. Matveev, J. Alnis, R. Pohl, Th. Udem, U.D. Jentschura, N. Kolachevsky, T. W. Hänsch, *Precision Measurement of the Hydrogen-Deuterium $1S-2S$ Isotope Shift*, Phys. Rev. Lett. 104 (2010) 233001.
- [Žá10] M. Žáková, Z. Andjelkovic, M.L. Bissell, K. Blaum, G.W.F. Drake, Ch. Geppert, M. Kowalska, J. Krämer, A. Krieger, M. Lochmann, T. Neff, R. Neugart, W. Nörtershäuser, R. Sánchez, F. Schmidt-Kaler, D. Tiedemann, Z.-C. Yan, D.T. Yordanov, C. Zimmermann, *Isotope shift measurements in the $2s_{1/2} \rightarrow 2p_{3/2}$ transition of Be^+ and extraction of the nuclear charge radii for $^{7,10,11}\text{Be}$* , J. Phys. G 37 (2010) 055107.
- [Av11] M. Avgoulea, Yu.P. Gangrsky, K.P. Marinova, S.G. Zemlyanoi, S. Fritzsche, D. Iablonskyi, C. Barbieri, E.C. Simpson, P.D. Stevenson, J. Billowes, P. Campbell, B. Cheal, B. Tordoff, M.L. Bissell, D.H. Forest, M.D. Gardner, G. Tungate, J. Huikari, A. Nieminen, H. Penttilä, J. Äystö, *Nuclear charge radii and electromagnetic moments of radioactive scandium isotopes and isomers*, J. Phys. G 38 (2011) 025104.
- [Co11] T.E. Cocolios, W. Dexters, M.D. Seliverstov, A.N. Andreyev, S. Antalic, A.E. Barzakh, B. Bastin, J. Büscher, I.G. Darby, D.V. Fedorov, V.N. Fedosseyev, K.T. Flanagan, S. Franchoo, S. Fritzsche, G. Huber, M. Huyse, M. Keupers, U. Köster, Yu. Kudryavtsev, E. Mané, B.A. Marsh, P.L. Molkanov, R.D. Page, A.M. Sjoedin, I. Stefan, J. Van de Walle, P. Van Duppen, M. Venhart, S.G. Zemlyanoy, M. Bender, P.-H. Heenen, *Early onset of ground-state deformation in the neutron-deficient polonium isotope*, Phys. Rev. Lett. 106 (2011) 052503.
- [Ma11] K. Marinova, W. Geithner, M. Kowalska, K. Blaum, S. Kappertz, M. Keim, S. Kloos, G. Kotrotsios, P. Lievens, R. Neugart, H. Simon, S. Wilbert, *Charge radii of neon isotopes over sd -shell*, Phys. Rev. C 84 (2011) 034313.
- [Nö11] W. Nörtershäuser, R. Sánchez, G. Ewald, A. Dax, J. Behr, P. Bricault, B. A. Bushaw, J. Dilling, M. Döbbsky, G. W. F. Drake, S. Götze, H.-J. Kluge, Th. Kühl, J. Lassen, C. D. P. Levy, K. Pachucki, M. Pearson, M. Puchalski, A. Wojtaszek, Z.-C. Yan, C. Zimmermann, *Isotope-shift measurements of stable and short-lived lithium isotopes for nuclear-charge-radii determination*, Phys. Rev. A 83 (2011) 012516.